

***Characterization of a membrane enzymatic complex  
for heterologous production of poly- $\gamma$ -glutamate in  
*Escherichia coli****

A dissertation submitted by

**Bruno Motta Nascimento**

in partial fulfillment of the requirements for the degree of

Doctor of Philosophy

in

*Biotechnology Engineering*

**Tufts University**

May 2021

Adviser: Nikhil U. Nair, Ph.D.

## Abstract

---

Poly- $\gamma$ -glutamic acid (PGA) is a polymer produced by many bacterial strains, with many distinct characteristics and applications. However, the enzymatic complex responsible for its synthesis has not been fully characterized yet, in native or recombinant contexts, leaving some room for further understanding its composition, structure and mechanism. Elucidating some of these properties would be crucial to develop more rational and improved designs of the enzyme and polymer. This study focuses on expressing the enzyme poly- $\gamma$ -glutamate synthetase (PgsBCAE, with its four subunits) heterologously in the *Escherichia coli* membrane and characterizing the localization, orientation, and activity of this heterooligomeric enzyme complex.

After optimization of expression and detection methods, we successfully expressed the enzyme in *E. coli* and produced the polymer with high molecular weight and minimal degradation. Deep-well microtiter batch cultures yielded approximately 13 mg/L of polymer. However, since we are using a heterologous host, it required further characterization of its localization at the membrane.

Microcopy imaging with fluorescent reporters allowed us to visualize the protein distribution along the cell. We observed that the subunits PgsB, C, A and E were all capable of directing the reporter to the *E. coli* membrane, despite the structural differences between the membrane of *E. coli* and the Gram-positive bacteria that naturally produce PGA. Complementary assays of PhoA activity and GFP fluorescence also provided information about the subunits C-terminal orientation across the cell membrane, confirming the prediction of transmembrane structures in the protein.

These results provide fundamental structural information on this poorly studied enzymatic complex and will aid future studies with this enzyme and engineering efforts to optimize its function, stability, or specificity.

## Acknowledgments

---

I would like to express my gratitude to my adviser, Professor Nikhil Nair, for giving me the opportunity to join his lab and guiding me through this research journey. His assistance and suggestions were of utmost importance for the completion of this work.

I also would like to thank my other thesis committee members: Professor Hyunmin Yi (Department of Chemical and Biological Engineering, Tufts University), Dr. Ajikumar Parayil (CEO & Founder at Manus Bio), Professor Stephen M. Fuchs (formerly at Department of Biology, Tufts University), and Professor Xiaocheng Jiang (Department of Biomedical Engineering, Tufts University). Our discussions were extremely helpful to overcome some challenges and steer towards the right direction.

Thank you to all my lab companions at the Synthetic Biology & System Bioengineering Lab for their collaboration. Their suggestions during experiments, cooperation during difficulties, or just late night talks, all were very helpful in the development of my work.

I also would like to thank my family and friends for their love and support, which were essential during this whole time. I would not have done it without them.

Finally, I must acknowledge the funding provided by CAPES Science without Borders (grant # 13015-13-3), Tufts University, and NIH (grant # DP2HD91798).

# Table of contents

---

<i>Abstract</i> .....	<i>ii</i>
<i>Acknowledgments</i> .....	<i>iv</i>
<i>Table of contents</i> .....	<i>v</i>
<i>List of Tables</i> .....	<i>viii</i>
<i>List of Figures</i> .....	<i>ix</i>
<i>Introduction</i> .....	<i>2</i>
<i>Dissertation scope and outline</i> .....	<i>4</i>
<b><i>Chapter 1: Polymers of biological origin and production of poly-<math>\gamma</math>-glutamate in bacteria (Literature review)</i></b> .....	<b><i>6</i></b>
1.1 Introduction.....	6
1.2 Polymers naturally synthesized by cells.....	7
1.3 Poly- $\gamma$ -glutamate synthetase enzymatic complex.....	8
1.4 Production of poly- $\gamma$ -glutamate in bacterial strains.....	11
1.5 Application of PGA and other poly amino acids of interest.....	14
1.6 Current trends in PGS/PGA research.....	16
<b><i>Chapter 2: Expression of poly-<math>\gamma</math>-glutamate synthetase in heterologous bacterial host and development of activity assay</i></b> .....	<b><i>18</i></b>
2.1 Introduction.....	18
2.2 Materials and methods.....	19
2.2.1 Strains and culture media.....	19
2.2.2 Cloning and expression.....	20
2.2.3 PGA production .....	21
2.2.4 Polymer detection .....	22

2.2.5	PGA Hydrolysis and HPLC .....	23
2.3	Results and discussion .....	25
2.3.1	Initial expression.....	25
2.3.2	Development of a high-throughput detection assay for PGA.....	27
2.3.3	Optimized expression.....	35
2.4	Chapter conclusions .....	40
<b>Chapter 3: Characterization of poly-<math>\gamma</math>-glutamate synthetase localization in <i>Escherichia coli</i>. 41</b>		
3.1	Introduction.....	41
3.2	Materials and methods .....	42
3.2.1	Bioinformatic analysis .....	42
3.2.2	Strains and culture media.....	42
3.2.3	Cloning and expression.....	43
3.2.4	Immunodetection of subunits.....	44
3.2.5	Microscopy of labeled subunits .....	45
3.2.6	Membrane orientation detection .....	45
3.3	Results and discussion .....	46
3.3.1	Homology model prediction of PGS subunits .....	46
3.3.2	Topological prediction and expression of individual PGA synthetase subunits	51
3.3.3	Localization of PGA synthetase subunits at the membrane.....	55
3.3.4	Topology of PGA synthetase subunits.....	60
3.4	Chapter conclusions .....	64
<b>Chapter 4: Conclusions and future work..... 66</b>		
4.1	General conclusions .....	66
4.2	Future directions .....	67

*Supplemental material* ..... 70  
*Bibliography* ..... 77

## List of Tables

---

<i>Table 1 - Organisms naturally producing poly-<math>\gamma</math>-glutamate of different molecular sizes and enantiomer composition. Adapted from Ashiuchi &amp; Misono (2003).</i>	9
<i>Table 2 - Heterologous expression of poly-<math>\gamma</math>-glutamate synthetase in <i>E. coli</i> and highest PGA yield achieved in liquid cultures</i>	13
<i>Table 3 - Bacterial strains used in this study.</i>	20
<i>Table 4 - Plasmids used in this study.</i>	21
<i>Table 5 - Plasmids used in this study.</i>	44

## List of Figures

---

<i>Figure 1 - Schematic structure of PGS complex at the cell membrane.....</i>	<i>10</i>
<i>Figure 2 - Reaction mechanism for PGA polymerization.....</i>	<i>11</i>
<i>Figure 3 – Expression of different constructs in E. coli MG1655(DE3) and BL21(DE3) and B. subtilis.....</i>	<i>26</i>
<i>Figure 4 - Cellular growth and PGA production in agar plates stained with methylene blue.....</i>	<i>30</i>
<i>Figure 5 - Spectrophotometric scan of methylene blue solution in the presence of different concentrations of pure PGA.....</i>	<i>31</i>
<i>Figure 6 – Detection of PGS in positively charged nylon membranes stained with methylene blue..</i> <i>.....</i>	<i>33</i>
<i>Figure 7 - Induction of PgsBCAE expression in all E. coli strains at different induction levels..</i>	<i>34</i>
<i>Figure 8 – PAGE detection of PGA precipitated from 24 h culture supernatant (LB medium) from B. subtilis and E. coli MGΔΔ with PgsBCAE construct on a low-copy vector.....</i>	<i>36</i>
<i>Figure 9 - Cetyl trimethylammonium bromide (CTAB) assay standard curve with pure PGA. ....</i>	<i>37</i>
<i>Figure 10 - HPLC of pre- and post-hydrolysis samples from (A) purified PGA from E. coli MGΔΔ PgsBCAE culture, (B) pure commercial PGA, and (C) pure L-glutamate. ....</i>	<i>38</i>
<i>Figure 11 – Detection by PAGE of PGA degradation by purified hydrolases (PgsD and GGT). PGA sample: produced by E. coli MGΔΔ pACYC-PgsBCAE. ....</i>	<i>39</i>
<i>Figure 13 – (A) MurD reaction mechanism and coordination with Mg<sup>2+</sup> ions at the ATP binding site. Adapted from Dementin et al. (2001). (B) Structural model of MurD (PDB: 5a5f) with UMA substrate and ADP. ....</i>	<i>48</i>
<i>Figure 14 – Structure model of E. coli FolC (PDB: 1W78) showing the substrate after phosphorylation (A), the ADP molecule (B), Mg<sup>2+</sup> ions (orange), and side chains coordinating the metal ions (red). Filled model shows the presence of two cavities, one for substrate access, and a second on the opposite side for ATP entrance.....</i>	<i>49</i>

Figure 15 – (A) Homology model of PgsB predicted by SWISS-MODEL using *E. coli* FolC as reference (PDB: 1OZ5). Highlighted in red are residues with possible interactions with Mg ions (S43, E112, H143, D145), blue is the N terminal, and yellow the C terminal. (B) Homology model of PgsB using *E. coli* murD as reference (PDB: 2UAG), where the putative catalytic site is hidden. ....50

Figure 16 - Topology prediction by CCTOP (Dobson, Reményi, and Tusnády 2015).....53

Figure 17- (A) SDS-PAGE of *E. coli* cell lysate expressing PgsBCAE subunits with a 6xHis-tag at the C-terminal (labeled with 'H' at legend). (B) Western blot of same samples using anti-6xHis antibodies.....55

Figure 18 - (A-D) Fluorescence microscopy of cells expressing individual subunits PgsA, C, E, and B, respectively, each with sfGFP at the C-terminus. Variants of PgsB are (E) without signal peptide (PgsB $\Delta$ 21) and (F) and with only the signal peptide (ssPgsB). (G) sfGFP alone as cytoplasmic expression control.....57

Figure 19 - Fluorescence microscopy of cells expressing pgsBCgAEr operon, where the PgsC subunit is linked to sfGFP/green and PgsE to mCherry/red, both at the C-terminal.....58

Figure 20 –Expression of PgsB and PgsB $\Delta$ 21 tagged with sfGFP at different induction levels of IPTG.....59

Figure 21 – Cell physiology of PgsBCAE at different induction levels of IPTG.....60

Figure 22 - (A) LB+X-Pho plates after induction with IPTG. (B) Relative fluorescence (RFU/OD<sub>600</sub>) of *E. coli* MG $\Delta$  strains expressing each full-length subunit with GFPuv fused at its C-terminus.....62

Figure 23 - Schematic representation of PgsBCAE localization at cell membrane. White circles indicate the amino acid location where reporter fusions were added.....64

**Supplemental Figures:**

Sup. Fig. 1 - Multiple sequence alignment by CLUSTAL O of PgsB from Bacilli (black labels) and other poly-amino-acid synthetases (red labels). The putative sites of interaction with ATP are highlighted in yellow.....73

*Sup. Fig. 2 – Homology models for each PgsBCAE subunit obtained with SWISS-MODEL server (Schwede et al. 2003).....74*

*Sup. Fig. 3 - Individual topology prediction by different server algorithms (HMMTOP, Memsat, Octopus, Philius, Phobius, Pro, Prodiv, Scampi-single, Scampi-msa, TMHMM, SignalP) (Dobson, Reményi, and Tusnádý 2015).....76*

*Characterization of a membrane enzymatic complex  
for heterologous production of poly- $\gamma$ -glutamate in  
*Escherichia coli**

## Introduction

---

The synthesis of renewable polymers in biological systems is not a new concept, since cells can create a large number of linear and branched polymers. Such polymers play the most diverse roles, either within a single cell or in a multicellular system: in example, cellulose provides structural support in individual plant cells, but may also be the constituent of the extracellular matrix of biofilms of various bacteria. Natural polymers have already been used extensively in the industry, such as silks, collagen, starches, xanthan, chitosan, polylysines, polyglutamates, and PHA, among others. However, the cellular machinery is limited, constraining the development of new polymers with different properties.

Recent advances in biotechnology have allowed researchers to manipulate the cell in many different levels, making it is possible to design new biosynthetic platforms for industrial application. Currently, the production of new biopolymers has be accomplished in the literature by different approaches, such as engineering microbial cell to produce new building blocks, which can be polymerized by the cell or by subsequent chemical process (Lee et al. 2011); using new enzymes that carry out new polymerizing reactions or modify the polymer by introducing functional groups (Matsumoto and Taguchi 2013; Gübitz and Paulo 2003); or reprogramming the translation apparatus (ribosome and related factors) to accept non-canonical amino acids (Des Soye et al. 2015; Hong, Kwon, and Jewett 2014).

In my research project, we intended to follow a different path to obtain new polymers. We aspired to use a naturally occurring enzymatic complex and evolve it *in vitro* to be to accept different building blocks as monomers and produce different types of polymers. We hypothesize that by

changing the enzymatic interactions with the substrate we would be able to switch to different substrates and produce polymers that until now are not produced by any biological system.

However, a rational design for this kind of protein evolution requires some minimal characterization of the system. Unfortunately for the chosen enzymatic complex of this dissertation, the poly- $\gamma$ -glutamic acid synthetase (PGS), little information has been obtained previously in the literature for its structure and activity. In order to move forward in the overall research goal of the laboratory, this dissertation takes the initial steps necessary to understand the production of poly- $\gamma$ -glutamic acid (PGA) in a heterologous host and the proper localization of the active enzyme within this bacterial cell.

## Dissertation scope and outline

---

The overall objective of this dissertation is to study a poorly characterized enzyme, the multi-subunit enzymatic complex of poly- $\gamma$ -glutamate synthetase (PGS), and to analyze the efficacy of expressing it in a non-natural bacterial host. The dissertation is organized into the following chapters:

### **Chapter 1: Polymers of biological origin and production of poly- $\gamma$ -glutamate in bacteria (Literature review)**

This section is a literature review on natural polymers (including poly- $\gamma$ -glutamate) synthesis, with emphasis on those produced in bacteria. I discussed previous studies on this biosynthesis and what the current developments are in this field.

### **Chapter 2: Expression of poly- $\gamma$ -glutamate synthetase in heterologous bacterial host and development of activity assay**

We isolated genes from *Bacillus subtilis*, encoded by the *pgsBCAE* operon, and cloned into *Escherichia coli* cells. We constructed different cassettes with combinations of the PGS subunits (BCAE, BCAE, BCE, BC, BA, B, A) and induced in *E. coli* strains for expression. At this initial point, we also tested different detection methods and attempted to develop a new assay for fast

detection of enzyme activity. Here we discuss all the attempts made and the final production yields achieved in deep-well plates cultures.

### **Chapter 3: Characterization of poly- $\gamma$ -glutamate synthetase localization in *Escherichia coli***

Based on prediction models of PgsBCAE protein, we constructed an array of reporter cassettes for verifying the correct localization in the heterologous host. Methods for protein detection, such as electrophoresis, western blotting, fluorescence microscopy, and enzymatic activity, were employed for this initial characterization of the enzymatic complex. We successfully observed some characteristics of this enzyme, which had not been published in the literature before.

### **Chapter 4: Conclusions and future work**

Here is a summary of all the work developed in this dissertation and suggestions on not only how this project could move towards the broader scope of research (changing the enzyme specificity for producing new polymers), but also how it could branch out to other types of projects.

# **Chapter 1: Polymers of biological origin and production of poly- $\gamma$ -glutamate in bacteria (Literature review)**

---

## **1.1 Introduction**

All living organisms can naturally produce some type of polymer, however only some of them can be efficiently harvested for industrial applications. The membrane-associated poly- $\gamma$ -glutamate synthetase (PGS) found in many species can simultaneously polymerize and secrete long polymers of glutamic acid by linking alpha amines to the adjacent gamma carboxylates. This first chapter offers a literature review on the biochemical synthesis of poly- $\gamma$ -glutamic acid (PGA), especially focused on the microbial sources, and how current research has directed its attention mainly to the polymer itself and not to the enzyme. The lack of material on the organization at the membrane level led us to focus this dissertation on characterizing a bit further the PGS enzyme.

With future goals seeking to change the specificity of this enzyme and catalyze the production of new polymeric materials, especially those currently produced only by chemical synthesis, a brief discussion on applications of other poly-amino acids is also included in this chapter.

## **1.2 Polymers naturally synthesized by cells**

Organisms are equipped with a variety of biochemical processes to produce many chemicals and materials, many of which are useful not only to the own cell, but also can be harvested for additional applications. Polymers are one of these products, and are formed by condensation and/or addition of building block monomers (Lee et al. 2011).

Microorganisms can efficiently produce a vast array of building blocks that can be polymerized in vivo, such as cellulose and polypeptides, or processed ex vivo to create polymers such as polyamides and polyesters. From the naturally produced microbial polymers, xanthan gum was the first one to be scaled up for industrial production (Kreyenschulte, Krull, and Margaritis 2014). Afterwards, many polymers and applications started developing: cyanophycin (hydrogels and nutrition), polylysine (waste treatment, drug delivery), bacterial cellulose (paper and food industry), alginate (cell immobilization), and many others (Shi, Xu, and Cen 2007; Kreyenschulte, Krull, and Margaritis 2014).

The current market still faces some challenges regarding the biological production of polymers. Higher production costs and expertise required for microbial production and process development/optimization at a high scale, when compared to crude extraction from plant matter or chemical processes, can hamper the broader adoption of microbial processes. For example, microbial production of polyhydroxybutyrate can be 5-10 times more expensive than chemical synthesis (Kreyenschulte, Krull, and Margaritis 2014). However, growing concerns with environmental impact and use of renewable sources had pushed investment and developments in biotechnological approaches. Genetic and metabolic engineering of microbial strains has also

enabled the adoption of new biological processes, increasing the yield of monomers/polymers (Tsuge et al. 2016; Lee et al. 2011).

This dissertation is particularly interested in the poly- $\gamma$ -glutamate polymer, naturally produced by some *Bacillus* species, which is further discussed in the following sections.

### **1.3 Poly- $\gamma$ -glutamate synthetase enzymatic complex**

Poly- $\gamma$ -glutamate synthetase is a multimeric enzyme present in some *Bacillus* species and a few other organisms (Table 1). While some other amide ligases are able to synthesize poly-glutamate with  $\alpha$ -amide linkages between the amino and  $\alpha$ -carboxyl group of L-glutamate (Hamano et al. 2013; Kino, Arai, and Arimura 2011), the PGS produces an unusual anionic polymer with  $\gamma$ -amide linkages, where the amino group reacts with the side chain carboxyl group. In its natural cell environment, poly- $\gamma$ -glutamate (PGA) functions as a cryoprotective material (similar to insect cryoprotectant sericin), protects against protease and pH stresses, and serves as nutrient storage (Makoto Ashiuchi and Misono 2003; M. Ashiuchi and Misono 2002).

*Bacillus* cultures that produce PGA usually have a highly viscous appearance and they have been used in Japan for a long time to produce a fermented soybean product called natto (M. Ashiuchi and Misono 2002). Each species and strain presents a different preference for glutamate enantiomer and molecular size distribution. *B. anthracis* has a PGA composed of only D-glutamate, while *B. halodurans* uses only L-glutamate for the polymer production. Other *Bacillus* species have a polymer with diverse composition, and the mechanism for substrate preference is

still unknown. During PGA production, a depolymerase enzyme also accumulates in the media, breaking down the polymer and producing a final PGA in the supernatant with varied molecular mass (Makoto Ashiuchi et al. 2001). *B. anthracis* has a different mechanism for releasing the polymer to the extracellular media. Glutamyltransferases anchor the PGA molecule directly to its peptidoglycan membrane by covalent bonds and creating a protective capsule for the microorganism (Candela and Fouet 2005).

*Table 1 - Organisms naturally producing poly- $\gamma$ -glutamate of different molecular sizes and enantiomer composition. Adapted from Ashiuchi & Misono (2003).*

Producer	Molecular mass (kDa)	Content (%)	
		D-Enantiomer	L-Enantiomer
<i>Bacillus subtilis</i> (natto)	10-1000	50-80	20-50
<i>Bacillus subtilis</i> (chungkookjang)	>1000	60-70	30-40
<i>Bacillus licheniformis</i>	10-1000	10-100	0-90
<i>Bacillus anthracis</i>	ND	100	0
<i>Bacillus megaterium</i>	>200	50	50
<i>Bacillus halodurans</i>	10-15	0	100
<i>Natrialba aegyptiaca</i>	>1000	0	100
<i>Hydra</i> nematocysts	3-25	0	100

A few research findings support the hypothesis that PGS is a membrane-associated protein, comprised of four subunits (PgsBCAE) (Makoto Ashiuchi 2013). The polymerization of glutamate by PgsB and the secretion of the growing chain by PgsC-PgsA-PgsE is hypothesized to occur simultaneously, as proposed by the schematic representation in (Figure 1). Further characterization the activity of some isolated complexes *in vitro* revealed that PGS could hydrolyze ATP into ADP. It was shown that the PgsBC subunit alone is sufficient for this hydrolysis of ATP. Therefore, it was hypothesized that PgsBC is responsible for phosphorylating the  $\gamma$ -carboxyl group, which

subsequently undergoes nucleophilic attack by an incoming amino group, while PgsA plays a role in translocating the growing chain through the membrane (Makoto Ashiuchi et al. 2001). However, PgsE appears to be non-essential for enzyme activity, and its role is unclear until present time (Yamashiro, Yoshioka, and Ashiuchi 2011).

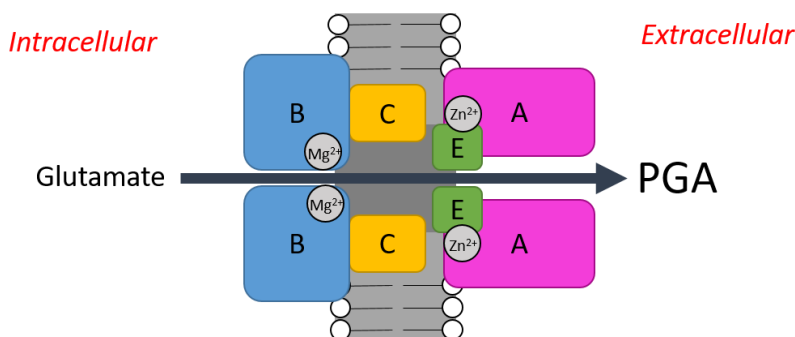


*Figure 1 - Schematic structure of PGS complex at the cell membrane. The intracellular D- or L- glutamate is phosphorylated at PgsB and the growing PGA traverses the membrane with the help of the other subunits. Mg<sup>2+</sup> and Zn<sup>2+</sup> have been shown to enhance PGA production, and possibly interact with PgsB and PgsE, respectively. Adapted from Makoto Ashiuchi (2013).*

The fact that the ATP hydrolysis generates ADP and not AMP supported the hypothesis that PGA is synthesized by an amide-ligation mechanism (Makoto Ashiuchi et al. 2001). Typical amide ligases contain a Rossmann-like fold similar to murein-biosynthetic enzymes and activate the C-terminal carboxyl residue of the polymers. This reaction mechanism that activates the growing polymer instead of the incoming substrate is also characterized by the lack of stereo-exactitude, resulting in the production of a polymer with varied DL-enantiomer composition (Makoto Ashiuchi 2013). It was determined *in vitro* that there was no phosphorylation activity of the enzyme towards monomers of glutamate, supporting the hypothesis that the enzyme might belong to the superfamily of Rossmann-type amide ligases, with a probable reaction mechanism proposed

in Figure 2 (Makoto Ashiuchi et al. 2001). It is also important to notice that in this proposed mechanism the PGA is not covalently bound to the enzyme at any stage (Makoto Ashiuchi 2013).

The reaction mechanism for PGA elongation has been proposed to start with step (A), when the phosphoryl group of ATP is transferred to the C-terminal carboxyl group of a growing chain, releasing ADP from the active site of the enzyme. Step (B) follows with the formation of an amide linkage via nucleophilic attack of the amino group of either a D- or L-glutamate on the phosphorylated  $\gamma$ -carboxyl group. In step (C), the polymer goes through multiple iterations of steps (A) and (B) within the enzyme until it is released to the extracellular environment (Makoto Ashiuchi 2013).

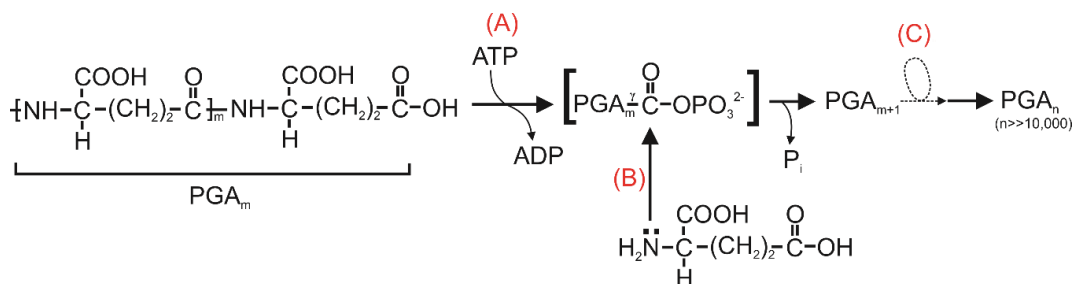


Figure 2 - Reaction mechanism for PGA polymerization. (A) The C-terminal carboxyl group is phosphorylated with the consumption of an ATP molecule. (B) A new glutamate molecule attacks the activated  $\gamma$ -carboxyl to form an amide linkage. (C) The polymerization continues to form PGA molecules with high molecular weight. Adapted from Makoto Ashiuchi (2013).

#### 1.4 Production of poly- $\gamma$ -glutamate in bacterial strains

For industrial application, most studies have relied on biosynthesizing PGA in *B. subtilis* strains.

However, the polymer productivity and quality can vary drastically depending on culture

conditions such as ionic strength, aeration, temperature and fermentation time (Makoto Ashiuchi 2013; Q. Wang, Wei, and Chen 2017). The isolation of new *B. subtilis* strains, such as chungkookjang that is able to produce PGA with higher molecular weight (> 2000 kDa) (Park et al. 2005), and culture media optimization has helped to increase the overall production yield to values up to 50 g/L of PGA (Makoto Ashiuchi 2013).

However, further characterization and engineering of the enzymatic complex requires the heterologous expression of the enzyme. Makoto Ashiuchi, Soda, and Misono (1999) group has been the first one to clone a PGS from *B. subtilis* in *E. coli* cells. In this initial work, they identified the gene operon responsible of PGA synthesis and determined that three subunits (B, C and A) were required for PGA production in *E. coli*.

Since then, a few other examples have shown the cloning of PgsBCA from *B. subtilis* (Jiang et al. 2006), *B. licheniformis* (Cao et al. 2013; N. Wang et al. 2011), and *B. amyloliquefaciens* (Cao et al. 2013, 2011). The enzymes were able to produce high molecular weight polymers, despite differences in membrane morphology between gram-positive bacilli and gram-negative *E. coli*. Table 2 summarizes all the heterologous work in *E. coli* with PGS that has been published so far in the literature.

Table 2 - Heterologous expression of poly- $\gamma$ -glutamate synthetase in *E. coli* and highest PGA yield achieved in liquid cultures

Host strain	Gene origin	PGA (g/L)	Ref.
<i>E. coli</i> JM109	<i>B. subtilis</i> IFO3336 ( <i>pgsBCA</i> )	0.024	(Makoto Ashiuchi, Soda, and Misono 1999)
<i>E. coli</i> JM109	<i>B. amyloliquefaciens</i> LL3 ( <i>pgsBCA</i> )	0.75	(Cao et al. 2011)
<i>E. coli</i> JM109	<i>B. licheniformis</i> NK-03 ( <i>racE</i> and <i>pgsBCA</i> )	0.603	(Cao et al. 2013)
<i>E. coli</i> JM109	<i>B. amyloliquefaciens</i> LL3 ( <i>racE</i> and <i>pgsBCA</i> )	0.645	(Cao et al. 2013)
<i>E. coli</i> BL21(DE3)	<i>B. subtilis</i> chungkookjang ( <i>pgsBCA</i> )	3.74	(Jiang et al. 2006)
<i>E. coli</i> JM109	<i>B. licheniformis</i> WBL-3 ( <i>pgsBCA</i> )	8.624	(N. Wang et al. 2011)

The development of some better tools to better engineer other hosts allowed recent studies in other strains. Xu et al. (2019) produced in *Corynebacterium glutamicum*, a strain that naturally produces high levels of glutamate, a PGA that they could control the amount of D- or L-glutamate used by combining different subunits of PgsBCAE from *B. subtilis* and *B. licheniformis* and their respective ratio, with a stereoselectivity of different strains ranging from 97.1% to 36.9% L-Glu. Halmschlag et al. (2019) not only attempted to control the stereochemical composition of the polymer, but also its molecular weight by using the same microbial chassis (*B. subtilis*) and expressing different combinations of enzymes from *B. subtilis*, *B. amyloliquefaciens* and *B. anthracis*. They produced PGA with defined properties such as composition (comprising of 3 to 60% D-Glu) and molecular weight ranging from 40 to 8500 kDa.

## 1.5 Application of PGA and other poly amino acids of interest

Homopoly-amino acids possess multiple applications due to their functional groups and properties. Among the most relevant ones it can be cited their use as biodegradable substitutes (as thermoplastics, fibers, biocompatible implants), hydrogels constituents with high water-absorption, flocculants, heavy metal adsorption agents for water treatment, cryoprotectants, antimicrobials, bitterness-relieving agents in food, thickeners, animal feed additives, osteoporosis-preventing factors, humectants, dispersants, drug deliverers, gene delivery vectors, and enzyme-immobilizing materials (Park et al. 2005; Numata 2015).

Poly- $\gamma$ -glutamate is considered non-toxic to humans and the environment, allowing its use in many application, ranging from the food industry (thickeners, humectants, bitterness-relieving agent) to the chemical (thermoplastics, hydrogels, fibers) and medical industries (bio-adhesives, immobilizing materials, drug delivery, gene vectors) (Makoto Ashiuchi and Misono 2003).

Aspartate could be considered the amino acid most similar to glutamate. Therefore, jumping from one to the other should be an easier task when changing the enzyme specificity. Poly-aspartate has applications as a dispersant, preventing the precipitation of salts in water cooling systems (Girasa and Wispelaere 2003) and wine preparations (Bosso et al. 2015). The presence of negative charges in the polymer prevents the crystal nucleation and growth for some inorganic salts. However, the only production process for poly-aspartate is by thermal polymerization, and no biosynthetic route has yet been characterized (Bosso et al. 2015).

Poly- $\epsilon$ -lysine is another polyamino acid of interest that consists of small L-lysine polymers (25-35 residues) with amide linkages between the  $\alpha$ -carboxyl group and the  $\epsilon$ -amino group. This

positively charged polymer presents antimicrobial activity against many microorganisms, and has been used as food preservative in many countries (Hamano 2011). Due to its low minimal inhibitory concentration against pathogens, the concentration present in food products is very low and has no effects in mammals (Shi, Xu, and Cen 2007). Other applications include drug delivery, enhancement of interferon inducers and inhibitory effect against pancreatic lipases. Even though a biosynthetic pathway exists in nature, with a non-ribosomal peptide synthetase (NRPS) mechanism in *Streptomyces albulus* (Shih, Shen, and Van 2006), no other bacterial strain or eukaryote have been found in nature producing this poly amino acid. Furthermore, longer chains are only available by chemical synthesis in the form of poly- $\alpha$ -lysine (Hamano 2011). Poly-arginine is another cationic polymer that presents similar properties to poly-lysine, such as drug/gene delivery (Holowka et al. 2007) and surface functionalization to prevent microbial growth (Mutschler et al. 2016). Gene transfer with these cationic polymers occurs mainly due to the electrostatic interactions with the DNA molecule and its membrane destabilizing properties (Munyendo et al. 2012).

In order to establish poly amino acids as a new functional and structural material, it necessary to develop a production process with high yield, low cost, and low environmental impact (Shi, Xu, and Cen 2007). Some chemo-enzymatic strategies have already been presented in the literature for the efficient synthesis of small poly amino acid (Numata 2015), but polymeric chains with high molecular weight still needs further development. Poly- $\gamma$ -glutamate is one of the few examples of polyamino acids produced naturally with high molecular weight. This motivates our work in understanding the PGS enzyme, to the point that in the future we could designing a new enzyme

capable of polymerizing novel poly amino acids with high molecular mass, overcoming the need for chemical synthesis.

## 1.6 Current trends in PGS/PGA research

As seen in the previous section, polyamino acids can have a diverse range of applications, causing the current focus of research groups to diverge significantly. For poly- $\gamma$ -glutamate, recent studies started focusing less on the producing enzyme (PGA), and more on chemical modification and overall strain engineering.

Chemical modifications with non-covalent cross-linkages in PGA was utilized to engineer coatings with antimicrobial properties and thermoplastics (Makoto Ashiuchi 2013; Makoto Ashiuchi et al. 2018). Complexation with other cationic surfactants to perform spontaneous coating of surfaces was also successful in producing a strong antimicrobial coat against *Staphylococcus aureus*, *Candida albicans*, and influenza viruses (Makoto Ashiuchi et al. 2015).

The microbial production needs to overcome some issues, such as degradation, regulation, dependence on glutamate for induction, growth stage dependence, and poor engineering tools for native hosts. Microbial strain engineering has succeeded in knocking out PGA hydrolase genes (*pgdS* and *ggt*) in *Bacillus licheniformis* RK14-46 to increase poly- $\gamma$ -glutamic acid production (Ojima et al. 2019) Engineering of *Corynebacterium glutamicum* for the de novo biosynthesis of tailored poly- $\gamma$ -glutamic acid using different PGS subunits achieved different stereoselectivity of the final polymer (Xu et al. 2019)

To further advance PGA production, in this dissertation we investigated the role and membrane localization of the different PGA subunits. This study focused on producing the PgsBCAE enzymatic complex from *B. subtilis* in *E. coli* and analyzing if it was enzymatically active and localized correctly to the membrane in this non-native host.

## Chapter 2: Expression of poly- $\gamma$ -glutamate synthetase in heterologous bacterial host and development of activity assay

---

### 2.1 Introduction

For industrial applications, most studies have relied on biosynthesizing PGA in *B. subtilis* (Park et al. 2005; Makoto Ashiuchi 2013; Q. Wang, Wei, and Chen 2017; Halmschlag et al. 2019) and other *Bacillus* species (Feng et al. 2015; Yoon et al. 2000; Xavier et al. 2019; Tian et al. 2014; Feng et al. 2017; Ogunleye et al. 2015), although there have been significant efforts in moving the complex to recombinant hosts such as *E. coli* (Cao et al. 2013; N. Wang et al. 2011; Cao et al. 2011; Makoto Ashiuchi, Soda, and Misono 1999; Jiang et al. 2006; Liu et al. 2019), *Corynebacterium glutamicum* (Xu et al. 2019), and even tobacco plants (Tarui et al. 2005). A major advantage of recombinant hosts is that PGA synthesis can be decoupled from native cellular regulatory processes and engineered for higher productivity, yield, stereochemical composition, and molecular weight. Further, the absence of any endogenous PGA hydrolytic enzyme (e.g., PgsD and GGT (Scoffone et al. 2013; Ojima et al. 2019)) ensures higher product stability during culture. Despite significant molecular and bioprocess engineering efforts, there have been few efforts focused on characterizing the structure, assembly, and function of this enzyme complex. Current research findings support the hypothesis that PGS is a membrane-associated protein comprised of four subunits – PgsB, PgsC, PgsA, and PgsE, as proposed previously (Makoto Ashiuchi 2013) – and that polymerization of glutamate occurs concurrently with secretion of the growing chain.

However, the role and membrane localization of the different subunits have not been well-characterized. Based on all these previous insights, our study initially focused on producing the PgsBCAE enzymatic complex from *B. subtilis* in *E. coli* and analyzing if it was enzymatically active in this non-native host.

## **2.2 Materials and methods**

### **2.2.1 Strains and culture media**

Bacterial strains used for this project are listed in Table 3. *Escherichia coli* NEB5 $\alpha$  competent strain was used during the cloning steps. *E. coli* BL21(DE3), MG1655(DE3) and MG1655(DE3) <sup>$\Delta$ recA, $\Delta$ endA</sup> was used for recombinant gene expression. Chemically competent cells were prepared by the calcium chloride/MES method.

Luria-Bertani (LB) media (VWR Life Science, #97064-110) was used for propagation and preservation of bacterial cells. In the case of solid medium, 18 g/L of bacteriological agar was added, and whenever the cells were transformed with plasmids, the appropriate antibiotic was added to the cooled medium at the recommended final concentration (chloramphenicol 25  $\mu$ g/mL or ampicillin 100  $\mu$ g/mL). Isopropyl  $\beta$ -D-1-thiogalactopyranoside (IPTG) was added for induction, and its concentration varied among experiments. Growth in liquid media was done in orbital shaker at 250 rpm and 37 °C, unless noted otherwise.

Table 3 - Bacterial strains used in this study.

Strain	Description	Source
<i>Escherichia coli</i> NEB5α	fhuA2 Δ(argF-lacZ)U169 phoA glnV44 Φ80 Δ(lacZ)M15 gyrA96 recA1 relA1 endA1 thi-1 hsdR17	New England Biolabs
BL21(DE3)	<i>E. coli</i> str. B, F <sup>-</sup> ompT gal dcm lon hsdSB(rB <sup>-</sup> mB <sup>-</sup> ) λ(DE3 [lacI lacUV5-T7p07 ind1 sam7 nin5]) [malB <sup>+</sup> ] <sub>K-12</sub> (λ <sup>S</sup> )	EMDMillipore
MG1655	<i>E. coli</i> str. K-12, F <sup>-</sup> λ <sup>-</sup> ilvG <sup>-</sup> rfb-50 rph-1	Lab collection
MG1655(DE3)	<i>E. coli</i> MG1655, λ(DE3)	Prather lab, MIT
MG1655(DE3) <sup>ΔrecA, ΔendA</sup>	<i>E. coli</i> str. K-12, F <sup>-</sup> λ <sup>-</sup> ilvG <sup>-</sup> rfb-50 rph-1, λ(DE3), Δ <i>recA</i> , Δ <i>endA</i>	Lab collection
<i>Bacillus subtilis</i> ATCC 6633	<i>B. subtilis</i> (Ehrenberg) Cohn	USDA-NRRL
168	<i>B. subtilis</i> Marburg mutagenesis, <i>trpC2</i>	USDA-NRRL

### 2.2.2 Cloning and expression

Plasmid extraction (miniprep) was performed using the E.Z.N.A.® Plasmid DNA Mini Kit I (OMEGA Bio-tek, #D6943-02). Horizontal DNA electrophoresis in agarose gel was performed in 1x TAE buffer according to (Sambrook and Russell 2001). Purification of DNA fragments from agarose gels used the MicroElute® Gel Extraction Kit (OMEGA Bio-tek, #D6294-02). DNA concentration was quantified by UV absorbance with the SpectraMax M3 microplate reader using a SpectraDrop Micro-Volume Microplate (Molecular Devices). DNA amplification with Taq DNA polymerase or Phusion® High-Fidelity DNA polymerase was performed according to manufacturer recommendations (New England Biolabs, Thermo Fisher Scientific). DNA digestion with restriction enzymes, DNA ligation with T4 DNA ligase, and DNA assembly with NEBuilder kit were done according to the manufacturer recommendations (New England Biolabs). DNA sequences of constructs were confirmed by sequencing with the appropriate primers, which was performed by GENEWIZ (Boston Lab, Cambridge/MA).

The *pgsBCAE* operon was amplified from *B. subtilis* 168 genome and used as template for all the constructs. In general, the PGS subunits were inserted in a pCDFlac or pACYC-Duet1 plasmid under control of a T7 promoter. Combinations of the subunits in an inducible operon structure generating the plasmids described on Table 4.

Table 4 - Plasmids used in this study.

Plasmids	Description	Source
pACYC-Duet1	Double multiple cloning site with T7 promoter/ terminator, chloramphenicol resistance ( <i>cat</i> )	EMDMillipore
pCDFlac	Derivative of pCDF-1b with lacUV5 promoter	Lab collection
pCDF-PgsBCAE	Complete PGS gene (BCAE) from <i>B. subtilis</i> 168 cloned at <i>NcoI</i> and <i>XhoI</i> sites of pCDFlac	This work
pCDF-PgsBCE	PGS subunits B, C, and E from <i>B. subtilis</i> 168 cloned at <i>NcoI</i> and <i>XhoI</i> sites of pCDFlac	This work
pCDF-PgsBC	PGS subunits B and C from <i>B. subtilis</i> 168 cloned at <i>NcoI</i> and <i>XhoI</i> sites of pCDFlac	This work
pCDF-PgsBA	PGS subunits B and A from <i>B. subtilis</i> 168 cloned at <i>NcoI</i> and <i>XhoI</i> sites of pCDFlac	This work
pCDF-PgsB	PGS subunit B from <i>B. subtilis</i> 168 cloned at <i>NcoI</i> and <i>XhoI</i> sites of pCDFlac	This work
pCDF-PgsA	PGS subunit A from <i>B. subtilis</i> 168 cloned at <i>NcoI</i> and <i>XhoI</i> sites of pCDFlac	This work
pACYC-BCAE	pACYC-Duet1 backbone with <i>pgsBCAE</i> operon	This work
pACYC-BCA	pACYC-Duet1 backbone with <i>pgsBCA</i> operon	This work
pACYC-BCE	pACYC-Duet1 backbone with <i>pgsBCE</i> operon	This work
pACYC-BC	pACYC-Duet1 backbone with <i>pgsBC</i> operon	This work
pACYC-BA	pACYC-Duet1 backbone with <i>pgsBA</i> operon	This work
pACYC-B	pACYC-Duet1 backbone with <i>pgsB</i> gene	This work
pACYC-A	pACYC-Duet1 backbone with <i>pgsA</i> gene	This work

### 2.2.3 PGA production

In 10 mL culture tubes, *E. coli* cells expressing PGS were grown in 5 mL of LB broth supplemented with 30 g/L L-glutamate, 10  $\mu$ M IPTG, and 25  $\mu$ g/mL chloramphenicol or 100  $\mu$ g/mL ampicillin. Cultures were incubated in an orbital shaker at 30 °C, 250 rpm, for 24h or 48h. *B. subtilis* strains were also grown in similar conditions, except without the addition of IPTG and antibiotic. Cultures

in 10 mL deep-well plates were performed similarly, except that plates were sealed and shaken at 700 rpm in a microplate shaker.

The PGA produced in the supernatant was either measured directly or after purified by a modified version of the copper precipitation method described by (Manocha and Margaritis 2010). In brief, 0.5 M  $\text{CuSO}_4$  was added to the supernatant and the solution was mixed by inversion and let stand for 1 h at room temperature. Tubes were centrifuged at 5,000 x g for 30 min and the pellets were later resuspended in phosphate buffered saline (PBS) pH 7.4 with EDTA 50 mM. The solution was dialyzed with SnakeSkin Dialysis Tubing 3.5 kDa molecular weight cut-off (Thermo Fisher Scientific, #68035) to remove salts, followed by drying in a vacuum centrifuge (Eppendorf Vacufuge Concentrator 5301).

#### **2.2.4 Polymer detection**

The concentration of dialyzed samples of PGA was determined by adapting the cetrimonium bromide (CTAB) turbidity method described by (Halmschlag et al. 2019). To every 100  $\mu\text{L}$  of sample it was added 50  $\mu\text{L}$  of CTAB solution (CTAB 0.1 M, NaCl 1 M) and let stand for 5 min, avoiding shaking of the plate that could disturb the turbid pellet. Turbidity of the resulting solution was measured at 400 nm. Based on a calibration curve using standards of pure PGA (Sigma-Aldrich, #G1049-100MG) in the concentration range of 0.25–0.025 g/mL, the concentration of  $\gamma$ -PGA from the culture supernatant was determined.

PAGE separation of PGA was done in a NuPAGE Bis-Tris 4-12% gel (Thermo Fisher Scientific, # NP0322BOX) and ran in 1x MOPS buffer (50 mM MOPS, 50 mM Tris, 0.1% SDS, 1 mM EDTA, pH 7.7) at 120 V for 2 h. The gel was washed twice with distilled wash for 5 min and stained with 0.03% methylene blue in 300 mM sodium acetate pH 5.2 for 15 min with a gentle rocker agitation. The gel was destained by multiple washes with deionized water until the background and clear against the PGA bands (Soto and Draper 2012).

PGA detection by dot blot with nylon membrane also uses a similar staining procedure. A positively charged nylon membrane (Amersham Hybond -N<sup>+</sup>, #RPN82B, GE Healthcare) was briefly dried at 37 °C and 2.5 µL each sample was applied to the membrane. The loaded membrane was dried again at 37 °C for 30 min and fixation was done with 60 % ethanol for 20 min. Ethanol was evaporated at 37 °C and the dry membrane was stained with 0.04 % methylene blue in methanol for 5-10 min. Destaining was done briefly with distilled water and followed by imaging.

### **2.2.5 PGA Hydrolysis and HPLC**

Purified PGA samples from *E. coli* cultures were hydrolyzed with 6 M HCl at 100 °C for 4 h in a vacuum sealed tube (Chemglass, #CG-4025-01). Acid was immediately removed with a vacuum centrifuge and pellet was resuspended in deionized water.

The presence of glutamate in the hydrolyzed samples was analyzed on an Agilent 1100 Series HPLC System, equipped with a Poroshell 120 HILIC-Z column (guard: 2.5 × 5 mm, 2.7 µm; main: 2.1 × 150 mm, 2.7 µm) and a diode array detector (Agilent, G1315B) measuring a signal at 338

nm wavelength (bandwidth = 10 nm) using reference wavelength 390 nm (bandwidth = 20 nm). Amino acid samples were derivatized with Fluoraldehyde *o*-phthaldialdehyde reagent (Thermo Fisher Scientific, #26025) prior injection in the system. The flow rate was constant and set at 0.3 mL/min. Solvents were run in a gradient condition with mobile phase A consisting of 10 mM ammonium acetate at pH 9.0 in water and mobile phase B consisting of 10 mM ammonium acetate at pH 9.0 in water:acetonitrile 1:9. After sample injection, mobile phases were run according to the following conditions: 0 – 2 min: 0 % A, 100 % B; 2 – 15 min: linear gradient to 30 % A, 70 % B; 15 – 16 min: linear gradient to 45 % A, 55 % B; 16 – 20 min: linear gradient to 0 % A, 100 % B; 20 – 25 min: 0 % A, 100 % B.

The enzymatic hydrolysis of PGA first required the production and purification of two known hydrolases (PgsD and GGT) *E. coli* cells with pACYC-PgsD or pACYC-GGT (both containing a 6xHis-tag at their C-termini) were grown in LB with chloramphenicol and induced with 0.1 mM of IPTG. Cells were washed and resuspended in 2500  $\mu$ L PBS, with the addition of 50  $\mu$ L lysozyme 5 mg/mL, 5  $\mu$ L DNaseI 5 mg/mL, and 2  $\mu$ L PMSF 1M. Samples were sonicated in an ice bath with BRANSON Sonifier 150 (10s ON, 1 min OFF, 5 min total ON, Amplitude 40 % with microtip). The suspension was centrifuged 3,000 x g for 15 min at 4 °C to remove cell debris, and the supernatant was collected. Soluble protein was purified via immobilized metal affinity chromatography (IMAC), with a gravity column containing TALON metal affinity resin (Takara Bio, #635502). A single elution of protein was achieved in elution buffer containing 500 mM imidazole. The buffer was exchanged with PBS containing using a Microsep 10 kDa Omega centrifugation spin column (PALL Corp). Purification was confirmed via SDS-PAGE and Western blot analysis. The purified enzymes were subsequently used for degrading PGA, incubating

samples in 0.1 M Tris buffer pH 7.8 added with 5 mM CaCl<sub>2</sub>, at 37 °C for 12h. The polymer degradation products of PGA were run in a PAGE gel and visualized with methylene blue staining, as described previously.

## 2.3 Results and discussion

### 2.3.1 Initial expression

The *pgsBCAE* gene was amplified by PCR from the genome of *Bacillus subtilis* 168 and cloned initially in a pCDFlac plasmid. During the initial cloning of these constructs in NEB5 $\alpha$ , it was noticed that cells that received the full construct (*pgsBCAE*) had a much lower transformation efficiency and a slower growth compared to others constructs. Even after transformation of other *E. coli* strains (Table 3), the same growth defect was observed, with the only exception being *E. coli* MG1655. The T7 expression system is probably carrying some burden to the cells, and since MG1655 does not contain the T7 RNA polymerase, it does not have a great impact on growth.

The insertion of correct sequence was confirmed by sequencing and the isolated clones for each construct were grown in liquid media to check for PGA production. This initial expression of PGS was induced with 0.5 mM IPTG and supplemented with 15 g/L L-glutamate. Culture tubes with 5 mL of media were incubated at 30°C and 250 rpm for 48 h.

The methylene blue staining of the gel was successful in detecting PGA in the *B. subtilis* supernatants and the *E. coli* transformed with the full PgsBCAE enzyme (Figure 3A). It is noticeable that the PGA produced by these strains has a high molecular weight, comparable to the

pure commercial PGA deemed to have a molecular weight greater than 750 kDa. The *B. subtilis* 6633 sample also seems to have a polymer with a broader molecular weight distribution, with a stained smear appearing at lower molecular weights. *E. coli* MG1655(DE3) with plasmid pCDF-PgsBCAE was the only one capable of producing PGA at a level that can be detected by this method. As noted before, this strain also presented impaired growth compared to wild type and other constructs.

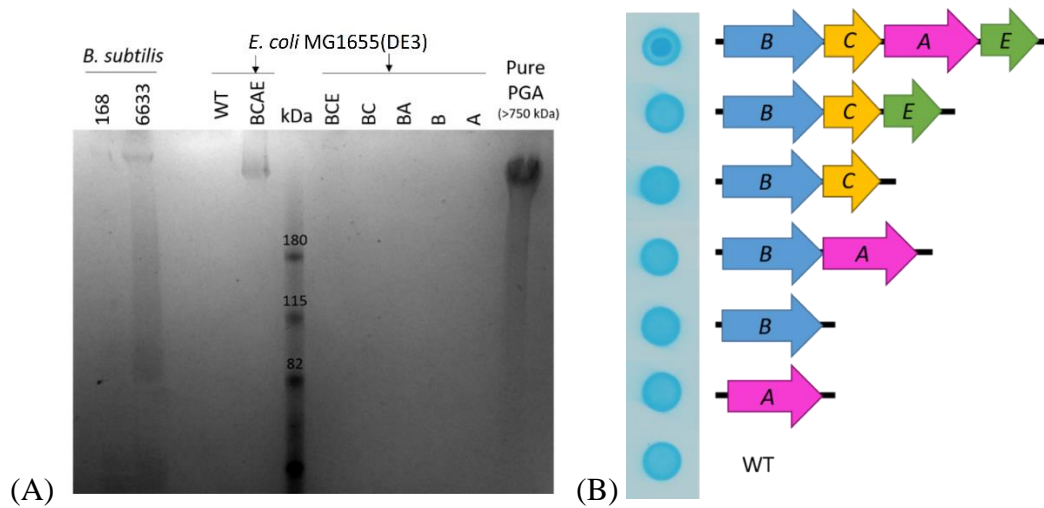


*Figure 3 – Expression of different constructs in E. coli MG1655(DE3) and BL21(DE3) and B. subtilis. (A) Detection of PGA in polyacrylamide gel electrophoresis of culture supernatant of B. subtilis (168 and 6633 strains) and E. coli MG1655(DE3) with each PGS subunit combination depicted in (B). WT – wild-type. Commercial purified PGA with molecular weight greater than 750 kDa was used as a positive control for methylene blue staining. Middle lane contains a protein MW marker for reference. (B) Dot blot detection of PGA produced from E. coli MG1655(DE3) with different cassettes.*

The same samples were later detected by the dot blot method (Figure 3B), which is much faster than electrophoresis and suitable for processing a large number of samples. The following section

of the text will discuss how this method was developed. It is worth noticing that only with the full *pgsBCAE* construct were we able to observe the characteristic staining of PGA.

### **2.3.2 Development of a high-throughput detection assay for PGA**

Even though the PAGE staining with methylene blue was successful in detecting poly- $\gamma$ -glutamate, this is a laborious and time-consuming assay. For enzyme engineering and library screening we would need an assay method that can be performed in high throughput. In the literature, PGA has been mostly detected after lengthy purification of samples and not in the crude cell broth.

PGA from *B. subtilis* samples is usually recovered from the culture by alcohol precipitation (ethanol, methanol or propanol) (Makoto Ashiuchi and Misono 2003). For a supernatant containing 1-2 % (w/v) PGA, approximately 75-80 % (v/v) of alcohol is used to precipitate the polymer. Since this purification strategy relies in the reduction of water activity around the polymer chain, it also co-precipitates other polymers, such as proteins and DNA, and ions. This usually requires dialysis of the samples for salt removal and lyophilization for sample concentration. Other precipitation methods use multivalent cations to precipitate PGA ( $\text{Cu}^{2+}$ ,  $\text{Mn}^{2+}$ ,  $\text{Al}^{3+}$ ,  $\text{Cr}^{3+}$  and  $\text{Fe}^{3+}$ ), reducing the volume of liquid necessary to handle. However, the later steps of salt removal and concentration are still necessary (Manocha and Margaritis 2010).

We have tested both purification methods with our constructed strains. However, both the *E. coli* strain producing PGA and the non-producing wild type presented a large amount of precipitated material. This is due mainly to the complex culture media being used (LB), which contains a high

amount of organic material. Switching to minimal media would overcome this problem. However, in this type of media we observed very poor growth and no detectable production of PGA. Since we had to stick to complex media, this precipitation, dialysis, and lyophilization steps were incompatible with a high-throughput assay. We needed an approach that could either detect PGA from the crude supernatant or from the initial precipitate.

The detection of PGA after purification is mostly reported in the literature by dry weight (N. Wang et al. 2011), size exclusion chromatography (Yoon et al. 2000; Scoffone et al. 2013), high performance liquid chromatography (HPLC) (Park et al. 2005), or polyacrylamide gel electrophoresis (M Ashiuchi et al. 1998; Yamashiro, Yoshioka, and Ashiuchi 2011; Ju et al. 2014). None of these methods are applicable for our aim, and other detection methods are necessary. Zeng *et al.* (2012) described a simple method for measuring aqueous solutions of PGA using UV absorption at 216 nm. Even though this method presents a linear range from 20 to 200 mg/L of PGA, it is sensitive to pH changes, and contaminating compounds (Zeng et al. 2012). When testing our cell samples, we were not able to get an accurate measurement using this UV absorption method.

Another possible method is the detection by CTAB turbidimetry, which was also tested in some of our samples. Cetyltrimethylammonium bromide (CTAB) is expected to bind to the PGA polymer and forms an insoluble complex, which can be quantified in a spectrophotometer at 400 nm (Makoto Ashiuchi 2011). However, our cells are cultivated in a complex media, which also precipitates in the presence of CTAB, making this alternative unfeasible for crude supernatant.

A few studies have also detected PGA with the use of polyclonal and monoclonal antibodies. Specimens of *Hydra* nematocysts (Szczepanek, Cikalá, and David 2002; Weber 1995) and *B. anthracis* (De Barun et al. 2002; Jang et al. 2013) have been detected by microscopy with labeled antibodies. Electron microscopy of these samples has shown that the antibodies bind at regular intervals of 36-38 nm along the PGA polymer (Candela and Fouet 2006). Even though this approach is presents high specificity, it is not cost effective for managing a large amount of samples.

Due to the anionic characteristic of the PGA polymer, the detection method that seems to be the most specific and with easy readout is the use of cationic dyes, such as methylene blue (MB), crystal violet and alcian blue. We have already described the use of methylene blue for PAGE gel staining in the previous topic. On this step, we desire to stain the PGA polymer without the electrophoretic separation.

The first attempt was incorporating the dye in agar plates, as shown in Figure 4. Methylene blue has a better contrast in minimal media (M9) compared to complex media (LB). However, as stated before, the cells already have diminished growth when the PGS genes are expressed. The limited resources in minimal media has prevented some strains from growing at all, even after longer periods of incubation.

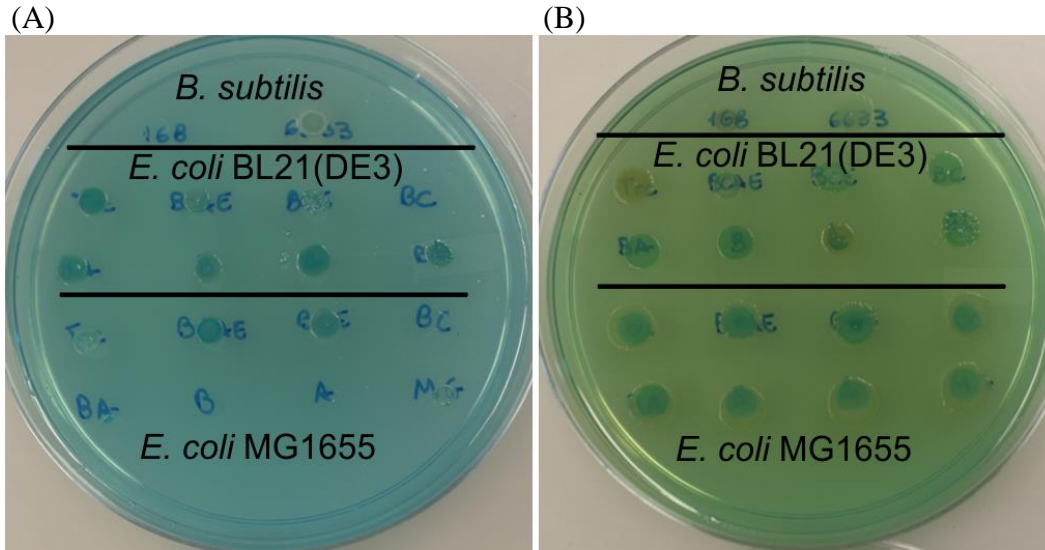
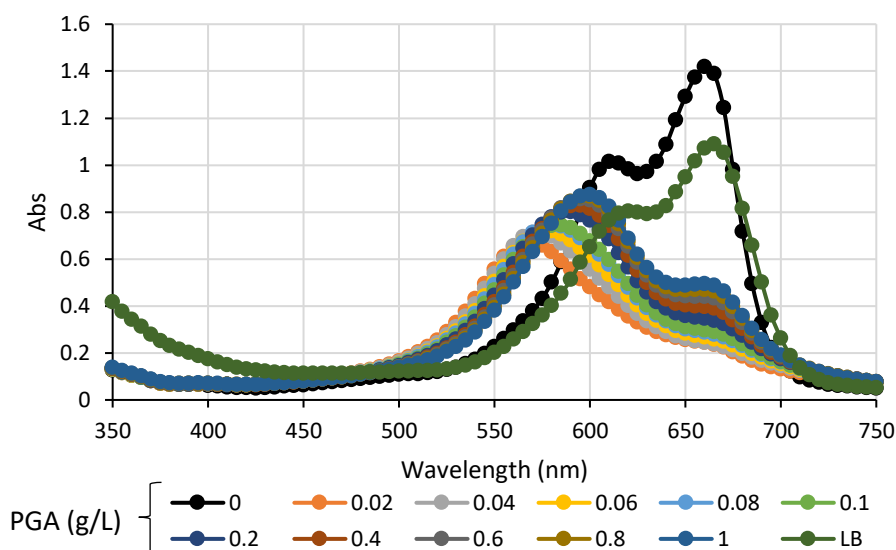


Figure 4 - Cellular growth and PGA production in agar plates stained with methylene blue. (A) M9 media or (B) LB media supplemented with 5 mg/L methylene blue, 1mM IPTG, and 15 g/L L-glutamate. Same OD600 of each culture was inoculated to the plates and incubated at 37°C for 2 days. Strain order starting from top left: *B. subtilis* 168 and 6633, *E. coli* BL21 (DE3) pTrc-PgsBCAE / pCDF-PgsBCAE / pCDF-PgsBCE / pCDF-PgsBC / pCDF-PgsBA / pCDF-PgsB / pCDF-PgsA / WT, *E. coli* MG1655 (same as BL21(DE3)).

The methylene blue present in the agar plates was also not successful in differentiating cells that contain PGA. We have tested different methylene blue concentrations and different staining procedures (MB present in the agar media, MB solution added to plate after growth and expression, or MB top agar layered over the plate after growth). None of those attempts were successful in staining PGA produced by cells. There was no consistency in the stained colonies, because even non producing strains got stained with MB. Colony lift in nylon membrane and staining with MB also produced unsuccessful results (data not shown).

Considering that the presence of cells is interfering with the measurement, we attempted to measure the secreted PGA directly in the supernatant of liquid cultures. The adsorption maximum

wavelength of methylene blue shifts to a shorter wavelength if PGA is present, in a phenomenon denominated metachromasia (Yamaguchi et al. 1996). Figure 5 shows the spectral scan of MB samples at different PGA concentrations. Once again, the method is successful in detecting PGA in a purified aqueous solution, as shown in the figure. However, when we used the culture broth as the diluent for PGA, the measurement is not as accurate. The presence of only LB media (dark green line) already causes a shift in the absorbance measurement.



*Figure 5 - Spectrophotometric scan of methylene blue solution in the presence of different concentrations of pure PGA. Also showing the observed shift when just LB interacts with methylene blue.*

Although we were not successful in quantifying accurately PGA in a crude broth with methylene blue, samples with PGA develop a purple color that can be inspected visually. We hypothesize that if we were able to remove the cells and some of the contaminating compounds prior to methylene blue staining, we would have at least a semi-quantitative method for MB staining.

It is worth mentioning that methylene blue could also stain other anionic polymers, such as DNA and RNA, that could be present in our biological samples. However, even when treating samples with DNaseI and RNase A, the results remained the same.

At this point, we also attempted to increase expression and cell growth by changing the *E. coli* strain and cultivation media. The different *pgsBCAE* plasmids were transformed in new *E. coli* strains and the cells were cultivated in a rich media denominated Magic Media (15 g/L LB broth, 5 g/L dextrose, 10 g/L yeast extract, 4 mL/L glycerol, 7.18 g/L K<sub>2</sub>HPO<sub>4</sub>, 1.53 g/L KH<sub>2</sub>PO<sub>4</sub>, 1.85 g/L MgSO<sub>4</sub>, 0.99 g/L (NH<sub>4</sub>)<sub>2</sub>SO<sub>4</sub>, 2 g/L Tris, 750 mL tap water/1L total media). This media containing higher amounts of carbon and nitrogen sources promoted better growth for all the producing strains.

For partial separation of the PGA polymer, we tried to develop a dot blot assay with the culture supernatant in a nylon membrane, which was positively charged and could interact with the negative charges of PGA to bind it. Two microliters of the cell culture were spotted on the membrane and after drying at room temperature it was washed for 15 min with ethanol 70%. We have attempted to perform the membrane staining similar to the PAGE protocol with MB (Yamaguchi et al. 1996) or the acridine orange staining described for *Hydra* samples (Szczepanek, Cikala, and David 2002), but both dyes presented a high background color and required a long destaining periods. After optimization of the methylene blue protocol (final protocol described in Materials and methods section), we were able to visualize differences between our producing strains (Figure 6). The presence of PGA creates a purple coloration in the membrane, while other media components create only a faint blue halo. This method is not as sensitive as other quantification methods listed above, nevertheless, it was the only one capable of detecting PGA in

the crude cell broth. As expected, both *B. subtilis* strains presented some PGA production, and were used as a positive control for the membrane staining. Surprisingly, the *E. coli* BL21(DE3) strain had the highest PGA production, even with its diminished growth compared to the other cultures.

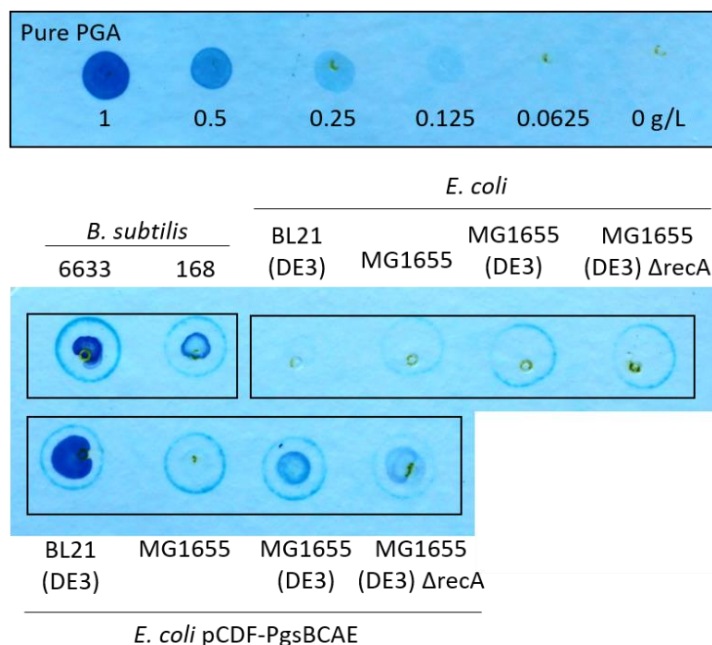


Figure 6 – Detection of PGS in positively charged nylon membranes stained with methylene blue. Bacterial strains were cultivated in test tubes with 5 mL Magic Media supplemented with 0.5 mM IPTG and 15 g/L L-glutamate for 48h at 30°C and 250 rpm.

We also tested the expression of the complete PGS at different induction level to find an optimal IPTG concentration for our producing cells (Figure 7). Even without induction, there seems to be a leaky expression of the enzyme, which may explain the slower growth of those cells. With only 10 μM of IPTG we can already detect a high amount of polymer with only 24 h of cultivation.

Higher IPTG concentrations reduced PGA concentration due to the impaired cell growth (data not shown) in those samples.

These encouraging results provided some growth/induction conditions and an easy detection assay for poly- $\gamma$ -glutamate. Even though the production titers were higher with *E. coli* BL21(DE3) cultures in Magic Media, the high copy of the pCDF-lac vector generated a lot of variability and instability of the membrane enzyme. Therefore we chose to make additional changes in the growth and expression strategy.

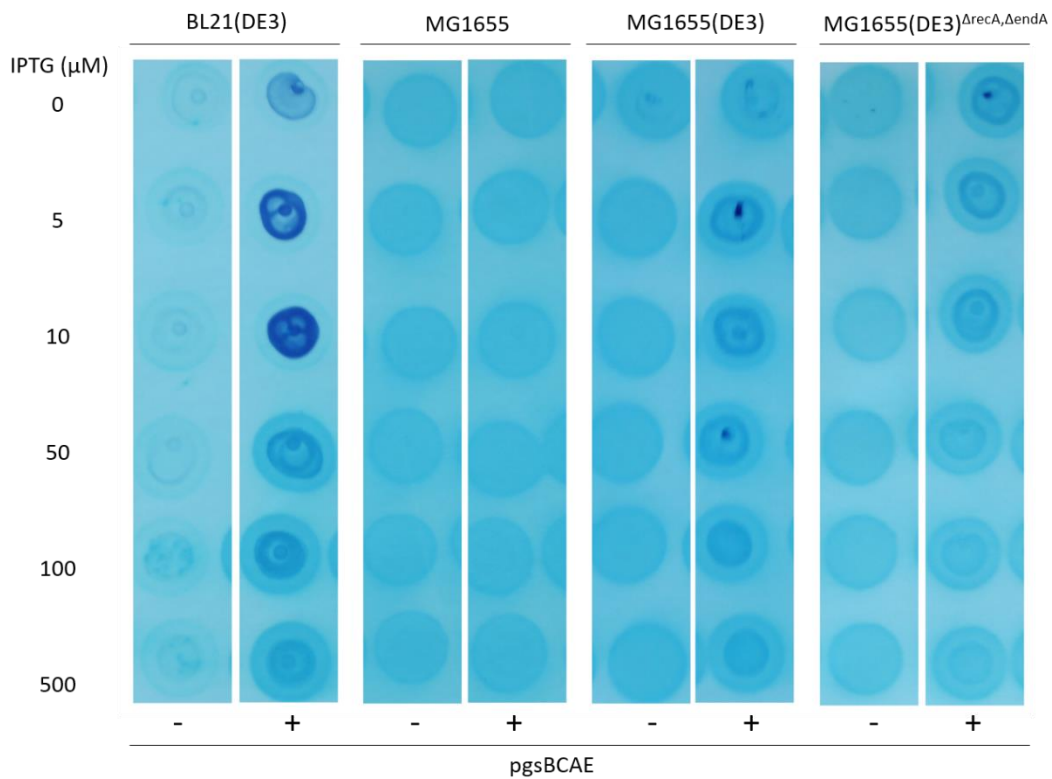


Figure 7 - Induction of PgsBCAE expression in all *E. coli* strains at different induction levels. Bacterial strains were cultivated in 96-well microplate with 150 μL Magic Media supplemented 15 g/L L-glutamate for 24h at 30°C and 1000 rpm.

### 2.3.3 Optimized expression

At this point, we decided that switching to a low copy vector would allow a more stable expression of PGS. The chosen backbone was pACYC-Duet1, which could still be induced with IPTG. Repeating the growth and induction experiments, we were able to obtain a good balance between growth and expression with the *E. coli* MG1655(DE3)<sup>ΔrecA,ΔendA</sup> (from now on referred as MGΔΔ) cells, which was singled out to continue on subsequent experiments.

Using LB media supplemented with 30 g/L glutamate, all PGS subunits (PgsBCAE, PgsBCA, PgsBCE, PgsBC, PgsBA, PgsB, or PgsA) were expressed in this strain and wild type *B. subtilis* strains (168 and 6633) were also used without antibiotics and induction. Cultivation conditions were scaled down to a 24-deepwell plate containing 5 mL of media, sealed with aluminum film, and agitated at 700 rpm in a microplate shaker. After 24 h, a fraction of the supernatant was collected and precipitated with a copper solution as described in materials and methods to obtain a clearer PAGE staining result (Figure 8). We found that the polymer produced by these bacteria have a high molecular weight (HMW), comparable to the pure commercial HMW PGA (>750 kDa). Since the PGA degrading enzymes are absent in the heterologous host, we can get a more consistence HMW with a smaller range of variation. In the future, it would be interesting to analyze these samples by size exclusion chromatography, to determine their precise molecular range.

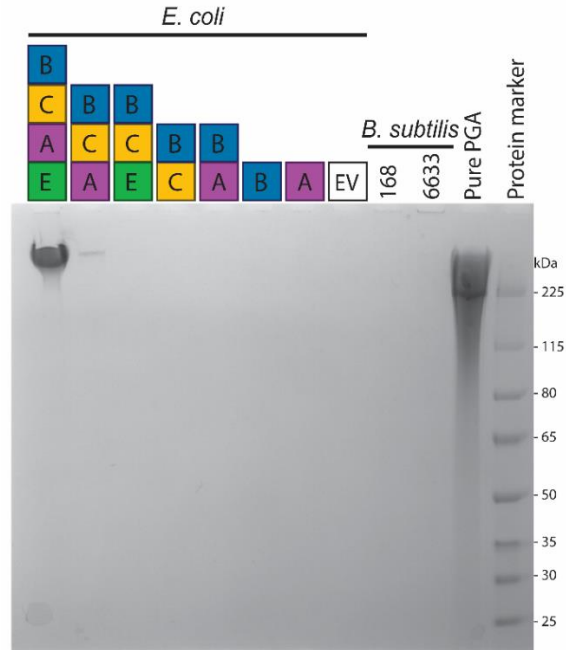


Figure 8 – PAGE detection of PGA precipitated from 24 h culture supernatant (LB medium) from *B. subtilis* and *E. coli* MGΔΔ with PgsBCAE construct on a low-copy vector. EV = empty vector negative control.

With purified PGA, we could also quantify the polymer by the CTAB method (Figure 9) and estimate a concentration of 13 mg/L and < 1.6 mg/L by PgsBCAE and PgsBCA expressing *E. coli*, respectively. These PGA titers are still much lower than the ones obtained in other *E. coli* cultures shown in Table 2. However, some of these works used larger culture strategies, sometimes even fed-batch conditions, to obtain higher PGA concentrations. We wanted to keep culture conditions at small scale, and therefore a compromise had to be made with productivity.

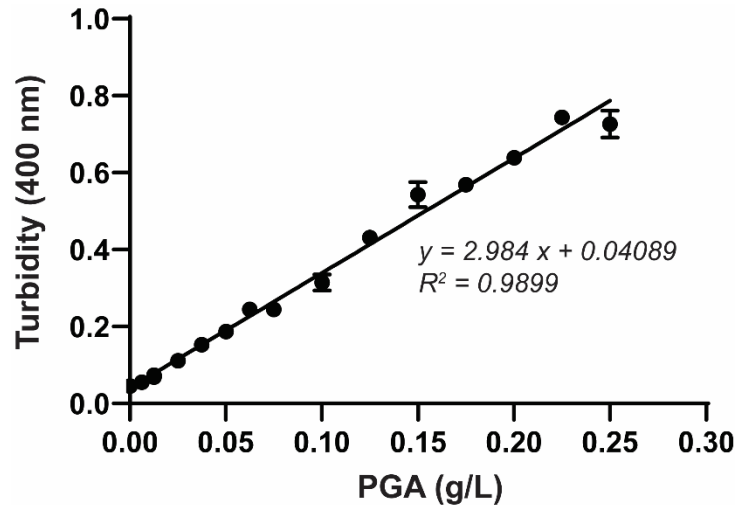


Figure 9 - Cetyl trimethylammonium bromide (CTAB) assay standard curve with pure PGA.

None of the other constructs tested in *E. coli*, nor wildtype *B. subtilis* 168, produced any detectable amounts of PGA under these conditions. These results also indicate that while PgsE is not essential for activity or processivity (Yamashiro, Minouchi, and Ashiuchi 2011; Yamashiro, Yoshioka, and Ashiuchi 2011; Makoto Ashiuchi, Yamashiro, and Yamamoto 2013), its presence enhances PGS activity in our culture conditions. The non-essentiality of PgsE corroborates with other published studies where only the PgsBCA subunits were used for expression (Cao et al. 2010; M. Ashiuchi and Misono 2002; Cao et al. 2011; Jiang et al. 2006).

To confirm that the band detected in the PAGE corresponded to PGA, the purified samples from a PgsBCAE expressing *E. coli* culture and a commercial PGA (Sigma-Aldrich, #G1049-100MG) were fully hydrolyzed with HCl at high temperature and analyzed by HPLC to compare to pure L-glutamate. The hydrolysate presented a single peak with an elution time similar to pure L-glutamate

(Figure 10), suggesting that the polymer we purified is indeed PGA and not any other negatively-charged polymer that may be interacting with the methylene blue stain.

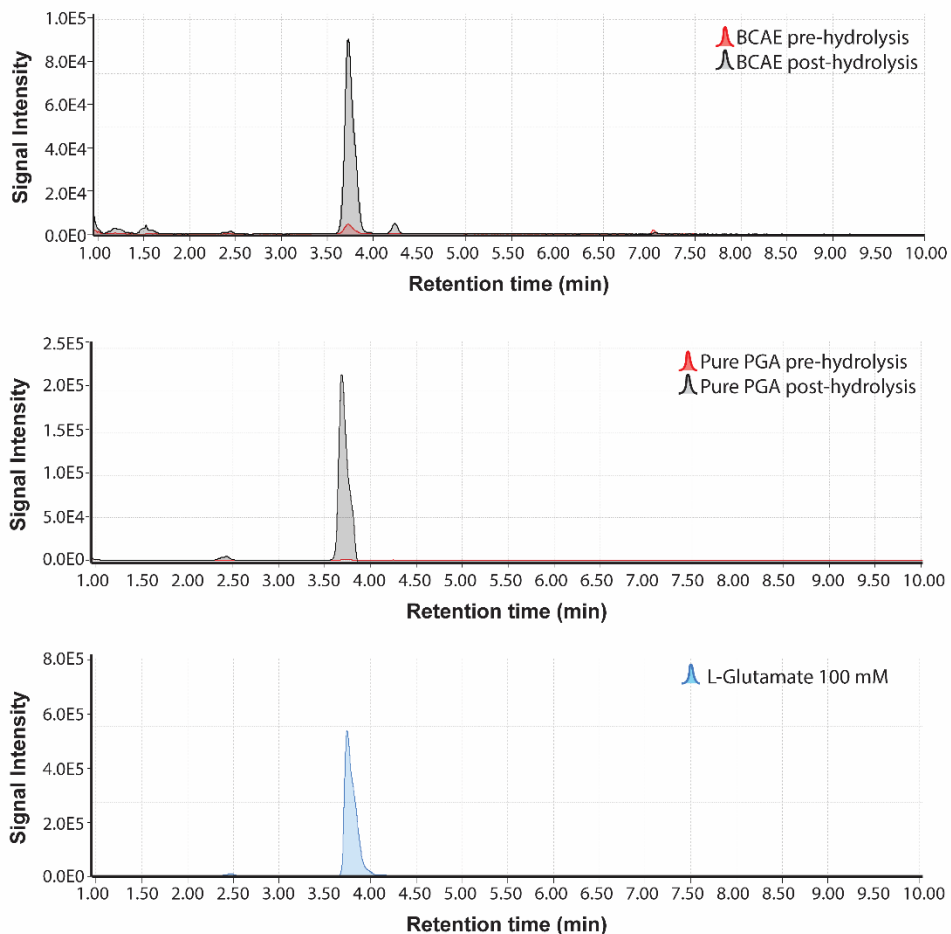
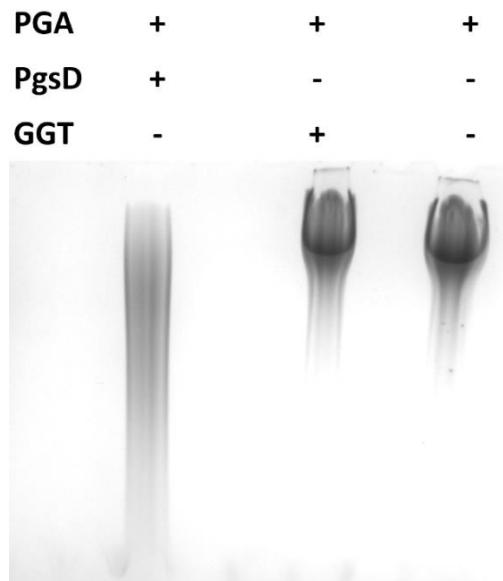


Figure 10 - HPLC of pre- and post-hydrolysis samples from (A) purified PGA from *E. coli* MGΔΔ *PgsBCAE* culture, (B) pure commercial PGA, and (C) pure L-glutamate.

An additional degradation of the polymer was performed by incubating PGA with its naturally occurring hydrolases, PgsD and GGT (Figure 11). In *Bacillus*, the *pgsD* gene (also referred as *pgdS* or *ywtD*) is located just downstream of the *pgsBCAE* operon. It is an endohydrolase, cleaving only the  $\gamma$ -glutamyl bonds between D- and L-glutamic residues of PGA (Feng et al. 2014). With

our enzymatic degradation result with PgsD, we can presume that the polymer we are producing is constituted by both D- and L-glutamate. Our previous HPLC analysis (Figure 10) could not distinguish between the enantiomers, with both having the same elution time. GGT is a glutamyltranspeptidase that transfers the  $\gamma$ -glutamyl end moiety to other peptides or water (in this case causing hydrolysis) (Kimura et al. 2004; Feng et al. 2014). *B. subtilis* GGT can generate both D- and L-glutamate as degradation products of PGA, but the precise hydrolytic mechanism is still unknown. *E. coli* also can naturally produce some form of GGT in its periplasm (Kimura et al. 2004). As we can see in our results, the PGA degradation is minimal when using just GGT. This is expected since at high molecular weight, the polymer has less ends to be attacked by the hydrolase. Usually, a good enzymatic degradation approach would consist to first use an endohydrolase to produce smaller chunks of the polymer, and subsequently introduce the exohydrolase.



*Figure 11 – Detection by PAGE of PGA degradation by purified hydrolases (PgsD and GGT). PGA sample: produced by E. coli MGΔΔ pACYC-PgsBCAE.*

## 2.4 Chapter conclusions

We successfully expressed the PgsBCAE membrane enzyme in a heterologous host, *E. coli*. The enzymatic complex was fully functional, and PGA was recovered from the supernatant of culture media. Even though production was low due to the small scale of experiments, achieving 13 mg/L of PGA, the polymer presented a high molecular weight and minimal degradation due to the absence of hydrolytic enzymes in *E. coli*. We further confirmed that the polymer was in fact PGA by analyzing its degradation products. Chemical and enzymatic hydrolysis of PGA produced by *E. coli* MG $\Delta\Delta$  pACYC-BCAE showed that the degradation products had glutamate monomers.

Throughout this phase of the research we could test different approaches on detection PGA. Most of the previously described methods require a pure polymer, achieved only by purification protocols that are impractical at large scale. We still adopted some of these detection assays (such as CTAB quantification and PAGE separation), but also developed a faster semi-quantitative method similar to a dot blot. Positively charged nylon membranes were spotted with the culture supernatant (surpassing the need for purification) and the presence of PGA adhered to the membrane was developed with methylene blue staining. Although this method requires consistent care during membrane handling, to avoid stripping everything out of the membrane, it provides a fast visual result for PGA production.

# Chapter 3: Characterization of poly- $\gamma$ -glutamate synthetase localization in *Escherichia coli*

---

## 3.1 Introduction

Poly amino acid synthetases are a small group of enzymes capable of catalyzing the linkage of amino acids independently from ribosomes. Among these, the membrane-associated poly- $\gamma$ -glutamic acid synthetase (PGS) found in many *Bacillus* species can simultaneously polymerize and secrete long polymers of glutamic acid. We showed in the previous chapter that expression of PGS in *E. coli* produced long chains of PGA. However, determining how the protein domains interact with the membrane is extremely important for characterizing proteins that do not have yet a high-resolution structure defined. This is the case for PgsBCAE.

Membrane proteins still present great challenges in structural biology studies. The complex environment of the cellular membrane is very difficult to isolate and stabilize for subsequent analysis of their 3-dimensional conformation (Postis et al. 2015). Until present date, no research group has been successful in obtaining the structure of the PGS complex.

Therefore, in this work we continue to analyze the PGS enzyme to refine some of its structural properties. Bioinformatic analysis of the sequences can show promising similarities with other known structures and already crystallized.

The use of detectable reporters can aid us into unveiling information about its membrane localization and orientation. We used sfGFP, GFPuv and PhoA tags and truncated versions of the PGS subunits to determine some of these characteristics, and constructed a possible orientation scheme for the whole PGS complex.

## **3.2 Materials and methods**

### **3.2.1 Bioinformatic analysis**

An initial prediction of each protein interaction with the cell membrane was performed with the Constrained Consensus TOPology prediction server (CCTOP) (Dobson, Reményi, and Tusnády 2015). It uses a combination of prediction methods (HMMTOP, Memsat, Octopus, Philius, Phobius, Pro, Prodiv, Scampi-single, Scampi-msa, TMHMM, SignalP) and generates a consensus topology with increased prediction accuracy. Homology model of the subunits were also constructed with the SWISS-MODEL server (Schwede et al. 2003).

### **3.2.2 Strains and culture media**

Bacterial strains used for this part of the project were already listed in Table 3. *Escherichia coli* NEB5 $\alpha$  competent strain was used during the cloning steps and *E.coli* MG1655(DE3) <sup>$\Delta$ recA, $\Delta$ endA</sup> was chosen for expression of tagged constructs. Chemically competent cells were prepared by the calcium chloride/MES method.

Luria-Bertani (LB) media (VWR Life Science, #97064-110) was used for propagation and preservation of bacterial cells. In the case of solid medium, 18 g/L of bacteriological agar was added, and whenever the cells were transformed with plasmids, the appropriate antibiotic was added to the cooled medium at the recommended final concentration (chloramphenicol 25 µg/mL or ampicillin 100 µg/mL). Isopropyl β-D-1-thiogalactopyranoside (IPTG) was added for induction, and its concentration varied among experiments. Growth in liquid media was done in orbital shaker at 250 rpm and 37 °C, unless noted otherwise.

### **3.2.3 Cloning and expression**

Cloning techniques have been discussed with details in the previous chapter. The *pgsBCAE* gene was amplified from *B. subtilis* 168 genome and used as template for all the constructs. In general, the PGS subunits were inserted in a pACYC-Duet1 or pET-Duet1 plasmid under control of a T7 promoter. Different combinations of the subunits with an operon inducible by IPTG generated the plasmids described on Table 5. Later, tagged versions of each subunit were created by adding to the C-terminus of each protein a 12 amino acid linker (GSAGSAAGSGEF) and different reporters (6xHis tag, sfGFP, mCherry, GFPuv, or phoA).

Table 5 - Plasmids used in this study.

Plasmids/Gene	Description	Source
pACYC-Duet1	Double multiple cloning site with T7 promoter/terminator, chloramphenicol resistance ( <i>cat</i> )	EMDMillipore
pET-Duet1	Double multiple cloning site with T7 promoter/terminator, ampicillin resistance ( <i>bla</i> )	EMDMillipore
pET-BCA	pET-Duet1 backbone with <i>pgsBCA</i> operon	This work
pET-BCE	pET-Duet1 backbone with <i>pgsBCE</i> operon	This work
pET-CAE	pET-Duet1 backbone with <i>pgsCAE</i> operon	This work
pET-BAE	pET-Duet1 backbone with <i>pgsBAE</i> operon	This work
pXXX-His	pACYC-Duet1 backbone, XXX= described operon or gene, 6xHis tag	This work
pXXX-mCherry	pACYC-Duet1 backbone, XXX= described operon or gene, mCherry tag	This work
pXXX-sfGFP	pACYC-Duet1 backbone, XXX= described operon or gene, sfGFP tag	This work
pXXX-GFPuv	pACYC-Duet1 backbone, XXX= described operon or gene, GFPuv tag	This work
pXXX-phoA	pACYC-Duet1 backbone, XXX= described operon or gene, phoA tag	This work
XXX	operon (BCAE, BCA, BCE, BC, BA), individual genes or their truncations	This work

### 3.2.4 Immunodetection of subunits

Subunits of PGS with 6xHis tags were detected by western blot. Expressing cells were lysed by sonication and proteins separated in a NuPAGE Bis-Tris 4-12% gel and ran in 1x MES buffer at 120V until loading dye reached the bottom of the gel. Protein staining was done with SimplyBlue SafeStain (Thermo Fisher Scientific, #LC6060) according to manufacturer instructions. Transference to a PVDF membrane for western blot was done with the Invitrogen Xcell II blot module. Membrane was blocked with 5% skim milk and antibody labeling used a primary mouse monoclonal anti-6xHis (Thermo Fisher, #MA1-21315) and a secondary rabbit anti-mouse IgG with HRP (Abcam, #ab6728). Chemiluminescence was detected with SuperSignal West Dura Extended Duration Substrate (Thermo Fisher Scientific, #34075) and photograph was captured in a gel documentation system.

### **3.2.5 Microscopy of labeled subunits**

Cells were pelleted and washed with 1x PBS solution for preparation of microscope slides. A thin 2 % (w/v) agarose pad was prepared on a glass slide and 1  $\mu$ L of cell suspension was added on top and air dried for about 5 min before placing a glass cover slip (Ke et al. 2016).

Imaging was performed with a DMI8 automated inverted microscope (Leica Microsystems, #11889113) equipped with a CCD camera (Leica Microsystems, #DFC300 G), and a TXR (Leica Microsystems, #11525310) and YFP (Leica Microsystems, #11525306) filter cube. For Z-stack images of fluorescence at the membrane, a blind deconvolution was performed using the LAS X software from Leica Microsystems.

### **3.2.6 Membrane orientation detection**

Fusions to PhoA are the most widespread periplasmic reporter fusions. Colonies expressing periplasmic PhoA fusions can be visually screened by supplementation of the agar medium with a PhoA-specific substrate 5-bromo-4-chloro-3-indolyl phosphate (X-Pho), yielding blue colonies when enzyme is active in the periplasm (Karimova and Ladant 2017).

Cells expressing the tagged subunit were streaked in a LB plate supplemented with 100  $\mu$ g/mL X-Pho and grown at 30 °C for 4 h. After this period of time, a filter disc containing 5 nmol IPTG was placed at the center and the cells continued to grow at 30 °C for 24 h. Plates were then photographed to check development of a blue color due to PhoA activity.

In opposition to PhoA, the GFPuv protein folds efficiently in the cytoplasm but does not form a stable structure when targeted to the periplasm by a Sec-type signal peptide. GFPuv does fold properly, however, when attached to cytoplasmic domains of inner-membrane proteins (Drew et al. 2002).

Cells expressing the tagged subunit were inoculated in 5 mL LB media and induced with 10  $\mu$ M IPTG at 30 °C for 4 h with shaking at 250 rpm. After this period of time, Optical density at 600 nm ( $OD_{600}$ ) and fluorescence (excitation: 485 nm/emission: 510 nm) were measured.

### **3.3 Results and discussion**

#### **3.3.1 Homology model prediction of PGS subunits**

The PGS enzyme structure still remains unresolved, but the role of some subunits can be speculated by some of its properties. It has been hypothesized in the literature that PgsB has an ATPase activity, PgsC has many transmembrane domains and aids in translocating the polymer, and PgsA-E have undefined function. PgsE subunit is thought to ‘moonlight’ – i.e., it has more than one role in the organism. It is believed that it helps in the maintenance of extrachromosomal DNA, as shown by Yamashiro, Minouchi, and Ashiuchi (2011) and Makoto Ashiuchi, Yamashiro, and Yamamoto (2013). The hypothesized role by Ashiuchi also places PgsE facing the cytosol.

The first study to propose a reaction mechanism for PGA synthesis was done by Troy (1973). He detected the ATPase activity of the PGS enzyme from *B. licheniformis* and hypothesized a reaction mechanism where L-glutamate is activated by ATP to form  $\gamma$ -glutamate-AMP + PPI.

Studies by Makoto Ashiuchi et al. (2001) and Urushibata, Tokuyama, and Tahara (2002) have later disproven this mechanism for *B. subtilis* by showing that PgsB uses ATP and releases ADP + Pi during the polymerization of poly- $\gamma$ -glutamate.

The fact that the ATP hydrolysis generated ADP and not AMP supported the idea that PGA is synthesized by an amide-ligation mechanism similar to murein-biosynthetic enzymes (Makoto Ashiuchi et al. 2001). Typical amide ligases contain a Rossmann-like fold and activate the C-terminal carboxyl residue of the polymers. This reaction mechanism that activates the growing polymer instead of the incoming substrate is also characterized by the lack of stereo-exactitude, resulting in the production of a polymer with varied DL-enantiomer composition.<sup>1</sup>

We attempted to perform *in vitro* reactions with PGS to detect ATP utilization but were successful. Difficulties in isolating an active membrane fragment with PGS prevented further pursuits in this area so we decided to focus on other aspects of PGS characterization.

Makoto Ashiuchi et al. (2001) have determined *in vitro* that they could not detect a glutamate molecule phosphorylated at the gamma position and, therefore, assumed that the growing chain of PGA was being phosphorylated in a similar way to other ligases with the reaction mechanism proposed in Figure 2. The ligase group in question is the Mur family involved in bacterial cell wall biosynthesis.

The peptidoglycan synthesis is a multi-step process that adds short polypeptide chains to UDPMurNac, which is subsequently transported through the membrane. MurC, MurD, MurE, and MurF each add respectively an Ala, Glu, meso-diaminopimelate, and Ala-Ala group to the growing chain by an ATP-dependent amide ligase mechanism (Smith 2006; Dementin et al. 2001). For

example, MurD catalyzes the addition of a glutamate to UDPMurNac-Ala (UMA) by phosphorylating the carboxyl group of alanine (Figure 12A). Magnesium ions coordinate at the ATP binding site with both the substrate and ATP, and residues at the entrance of the active site (Figure 12B, red) allow the access of a glutamate molecule for ligation to occur (Dementin et al. 2001).

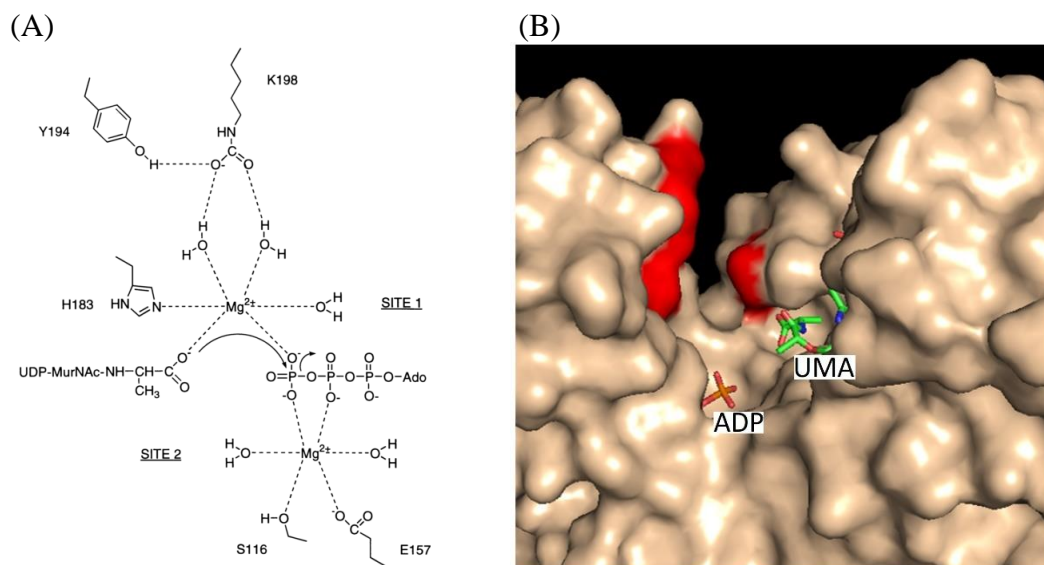
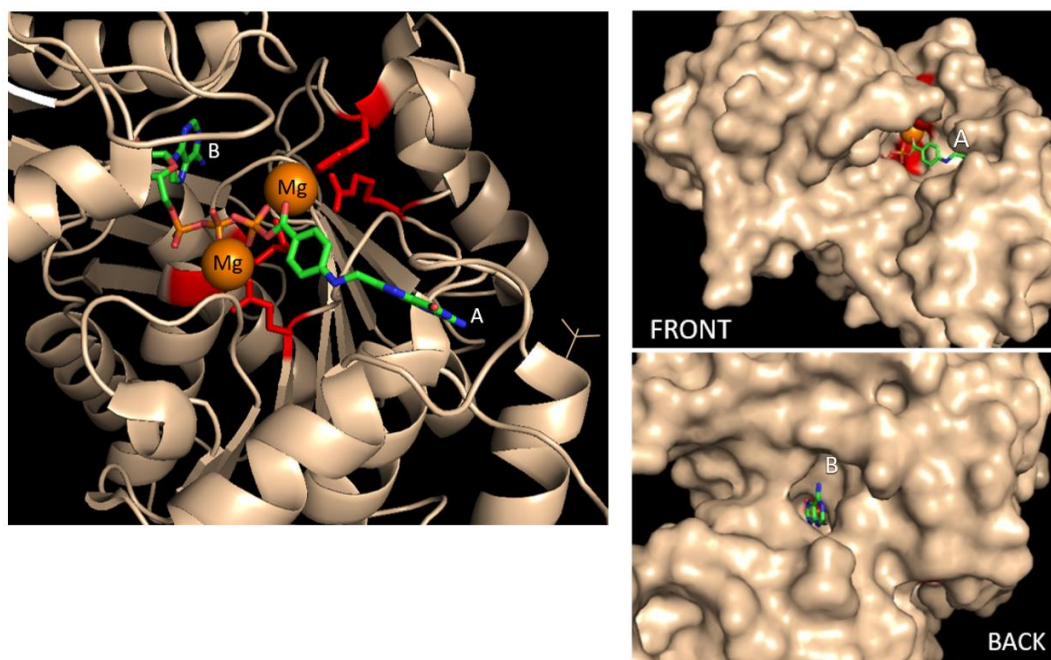


Figure 12 – (A) MurD reaction mechanism and coordination with Mg<sup>2+</sup> ions at the ATP binding site. Adapted from Dementin et al. (2001). (B) Structural model of MurD (PDB: 5a5f) with UMA substrate and ADP. Highlighted in red are residues K348, D182, and T321 involved in orienting the incoming glutamate for a nucleophilic attack.

We initially performed a sequence alignment by ClustalO (Sievers et al. 2011) of PgsB with *E. coli* Mur family and FolC proteins and observed some conserved motifs related the ATP binding site (Sup. Fig. 1). Construction of PgsB homology structure model with SWISS-MODEL server (Schwede et al. 2003) also presented high similarity and sequence coverage to proteins in the FolC and Mur ligase family (Sup. Fig. 2). These analyses are consistent with previous studies that PgsB

is homologous to other amide ligases and is the subunit responsible for catalysis (Makoto Ashiuchi et al. 2001).

The PgsB homology model had moderate similarity (~29 %) and sequence coverage (~80 %) with *E. coli* FolC (PDB: 1O5Z), MurD (PDB: 2UAG), and MurF (PDB: 1GG4). One main characteristic of these amide ligases is the presence of two cavities in the protein (Figure 13), one for ATP entrance, and the other on the opposite side for substrate access. The conserved residues that showed up from sequence alignment are the same ones that coordinate with  $Mg^{2+}$  at the catalytic site. Only the homology model of PgsB based on FolC was able to show a cavity that goes through the whole enzyme (Figure 14A). Other models showed no or limited access to the catalytic site (Figure 14B).



*Figure 13 – Structure model of E. coli FolC (PDB: 1W78) showing the substrate after phosphorylation (A), the ADP molecule (B),  $Mg^{2+}$  ions (orange), and side chains coordinating the metal ions (red). Filled model shows the presence of two cavities, one for substrate access, and a second on the opposite side for ATP entrance.*

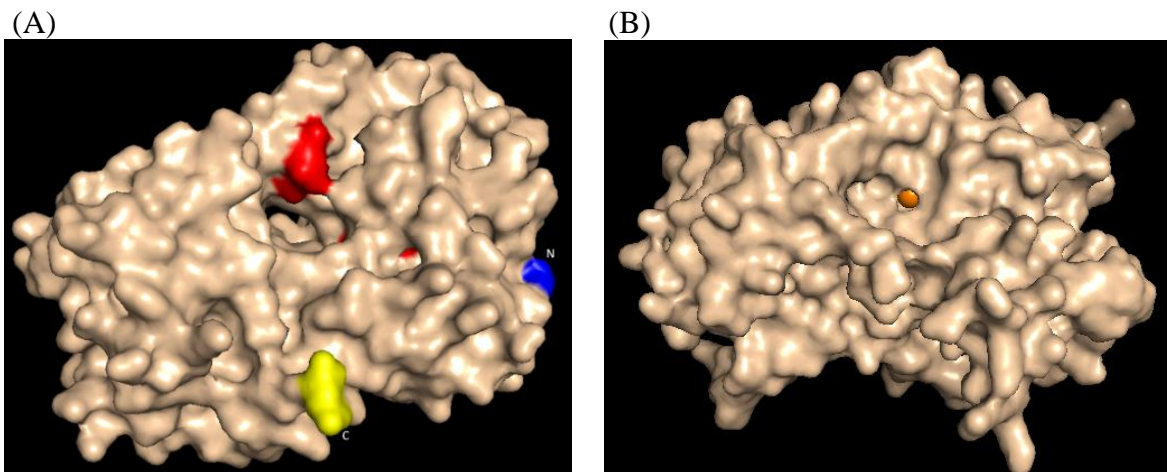


Figure 14 – (A) Homology model of PgsB predicted by SWISS-MODEL using *E. coli* FolC as reference (PDB: 1OZ5). Highlighted in red are residues with possible interactions with Mg ions (S43, E112, H143, D145), blue is the N terminal, and yellow the C terminal. (B) Homology model of PgsB using *E. coli* murD as reference (PDB: 2UAG), where the putative catalytic site is hidden.

The other PGS subunits presented less homology during alignment and model construction (Sup. Fig. 2). Urushibata, Tokuyama, and Tahara (2002) mention that PgsC presents certain similarity to the putative erythromycin transporter SmpA. Erythromycin resistance in *Staphylococcus epidermidis* is conferred by MsrA, a protein that contains similar ATP binding domains to an ABC transporter. However, this protein does not have any transmembrane portions. On the vicinity of the *msrA* chromosomal gene it was found another ORF that encodes for SmpA, a putative protein with many transmembrane regions that could possibly function in conjunction with MsrA (Ross et al. 1995; Reynolds, Ross, and Cove 2003). This interaction mechanism of MsrA and SmpA could be similar to the hypothesized role of PgsB and PgsC.

PgsA homology model usually presented hits with nucleases, but with lower sequence identity (~27 %) and coverage (~60 %). PgsE, due to its small size (55 aa), had only a couple of hits that mostly directed towards the presence of an alpha-helix structure.

### **3.3.2 Topological prediction and expression of individual PGA synthetase subunits**

Membrane insertion/translocation in *E. coli* usually occurs with the Sec, TAT or YidC pathway. The Sec pathway is the most common bacterial secretion mechanism, and translocation can either occur co-translationally (SRP) or post-translationally (SecA, SecB). The YidC pathway can work in cooperation with the Sec pathway proteins but can also function independently. The last mechanism uses the TAT pathway, which recognizes the signal peptide SRRxFLK and translocates proteins that are folded in the cytosol (Kolayarattil 2013; Pugsley 1993; Carlos et al. 2001). Cleavage of the signal peptide usually occurs but is not required after translocation through the membrane. The most common signal peptidases in gram-negative bacteria are: LepB (SPase I), which recognizes small amino acids at positions -1 and -3 (usually A or G) and turn-inducing amino acids at position -6 (G or P) with respect to the cleavage site; LspA (SPase II), which recognizes shorter signal peptides with more hydrophobic residues, no G or P at position -6, have a leucine at position -3, and cleaves proteins with a cysteine immediately after the cleavage site; and type IV prepilin peptidase, which cleaves the signal sequence at the cytoplasmic side of the membrane (Pugsley 1993).

It is unclear if any of the PGS subunits follow these secretion mechanisms. PGS subunits B and C contain a sequence that could possibly be regarded as a signal for secretion but does not appear to

have a recognizable cleavage site. It is known that SignalP, for example, does not predict well signal peptides that are left uncleaved (Kihara 2017). The signal peptide prediction also raises the question if PgsB is just associated with the membrane on the cytosol side or the signal fully translocates it to the periplasm.

The amino acid sequence of each PGS subunit was analyzed by different prediction tools in CCTOP to attest the presence of possible signal peptides and transmembrane regions. Due to the nature of each prediction algorithm and the training set that each of them uses, CCTOP compiles all results and outputs a probable topology for the sequence (Figure 15 and Sup. Fig. 3). The algorithm predicted a signal peptide for PgsB and PgsC but only presence of a transmembrane domain for PgsA and PgsE. Overall, this indicates that there is a high probability of co-localization of these proteins at cell membrane.

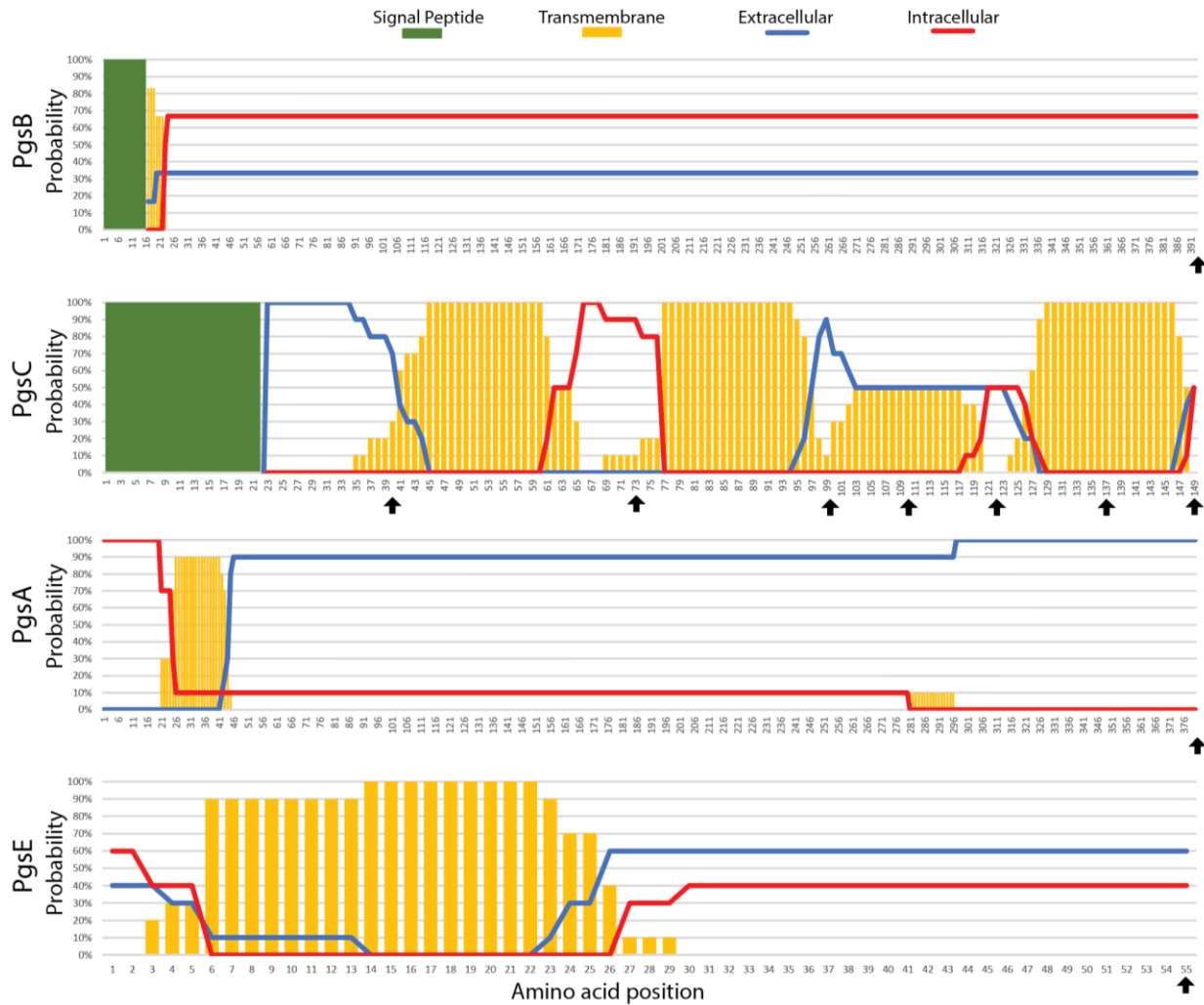


Figure 15 - Topology prediction by CCTOP (Dobson, Reményi, and Tusnády 2015). Each PGS subunit was analyzed individually by multiple prediction algorithms, and CCTOP combined the probability of each amino acid being intracellular, transmembrane, extracellular, or part of a signal peptide. Black arrows indicate residues where fusions are constructed.

To confirm the correct localization of these proteins in *E. coli*, individual PGS subunits were linked to a 6xHis tag for detection. Cells expressing tagged subunits were lysed and the soluble fractions (containing the soluble cytoplasmic proteins and small membrane fractions) and analyzed by SDS-PAGE and Western Blotting. All proteins have the expected size (PgsB: 44 kDa, PgsA: 43 kDa,

PgsE: 7 kDa), except for PgsC (16 kDa), which was not detected (Figure 16). From the sequence analysis (Figure 15), we expect PgsC to have a lot of interactions with the membrane, which likely hinders proper immunodetection within the soluble fraction. Interestingly, even though PgsA and PgsE are expected to have significant transmembrane interactions, we were able to detect them in the soluble fraction, suggesting relatively weak membrane anchoring.

We also prepared an additional construct of PgsB designated PgsB $\Delta$ 21, which does not contain the predicted 21 amino acid N-terminal signal peptide. We expect that this variant of the protein to not be directed to the membrane and remain in the cytoplasm. We were also able to detect C-terminally tagged PgsA as part of operon structure (*pgsBCAE* and *pgsBCA*), indicating that presence of other subunits does not occlude the tag. The presence of these proteins in the soluble fraction of the lysate indicate that they are not forming inclusion bodies inside the cell, which is important to note when interpreting that the subsequent microscopy studies.

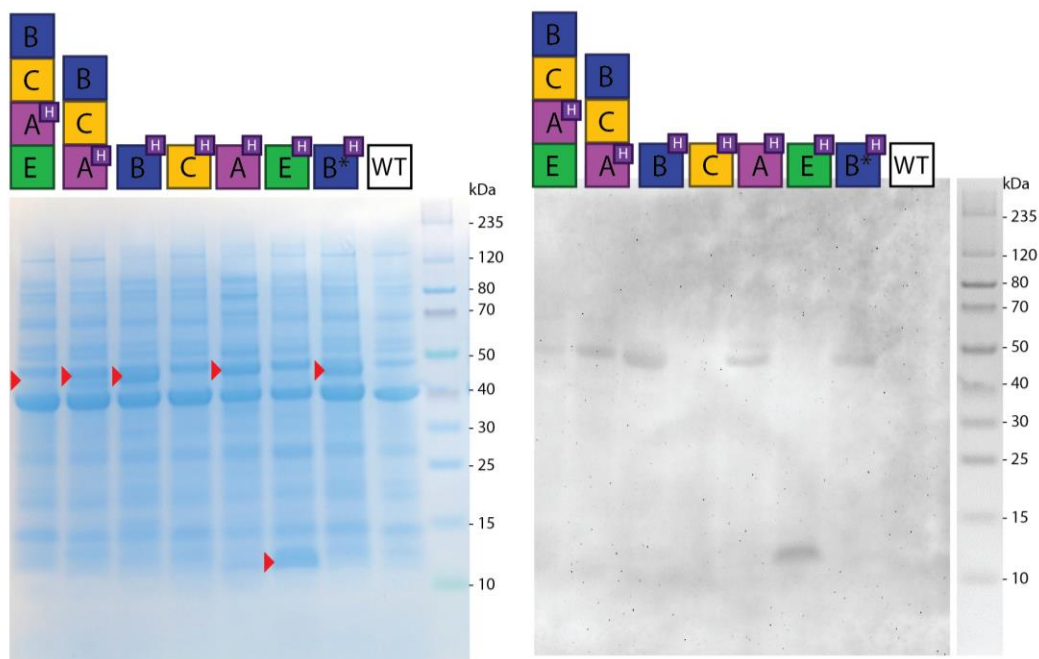


Figure 16- (A) SDS-PAGE of *E. coli* cell lysate expressing PgsBCAE subunits with a 6xHis-tag at the C-terminal (labeled with 'H' at legend). Red arrows indicate proteins present in the recombinant strains when compared to *E. coli* with empty vector control (EV). (B) Western blot of same samples using anti-6xHis antibodies.

### 3.3.3 Localization of PGA synthetase subunits at the membrane

Little has been attempted to detect the correct orientation of these proteins in the membrane. Membrane association of PGS has only been previously verified by membrane recovery after lysis and detection of either ATPase activity (for PgsB) or SDS-PAGE/Western bands (Makoto Ashiuchi et al. 2001; Urushibata, Tokuyama, and Tahara 2002; Makino et al. 1989; Feng et al. 2015).

Fusing each subunit with a fluorescent protein (sfGFP) enabled us to visualize how the different subunits localize in the cell. Superfolder GFP (sfGFP) is a highly efficient and stable folding variant, forming a folding intermediate that prevents the cysteine residues from forming disulfide bonds in the periplasm (Dammeyer and Tinnefeld 2012). Therefore, it fluoresces regardless of whether the C-terminal is exposed to the cytoplasm or periplasm. We fused each of the four subunits at their C-terminal to sfGFP and also created two variants of PgsB – one lacking the initial signal peptide (PgsB $\Delta$ 21-sfGFP) and another with just the signal sequence (ssPgsB-sfGFP). The localization of full-length PgsB fusion as well as the signal peptide only fusion is evident at the membrane (Figure 17D, F), especially when compared to the N-terminally truncated (PgsB $\Delta$ 21) variant (Figure 17E), where fluorescence is diffuse throughout the cytoplasm. For PgsC, PgsA, and PgsE we also note membrane localization, albeit with lower fluorescence intensities compared to PgsB (Figure 4A–C).

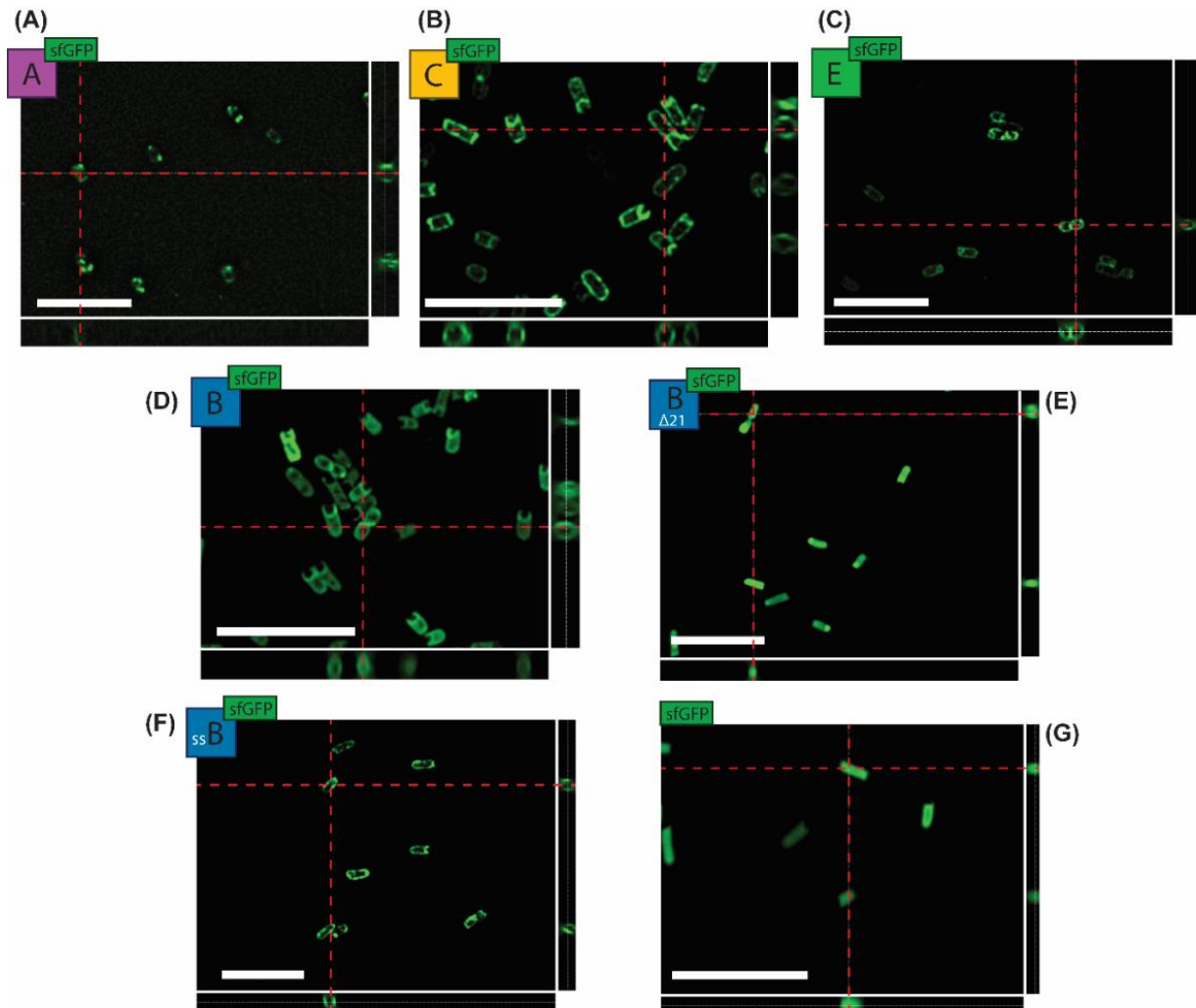
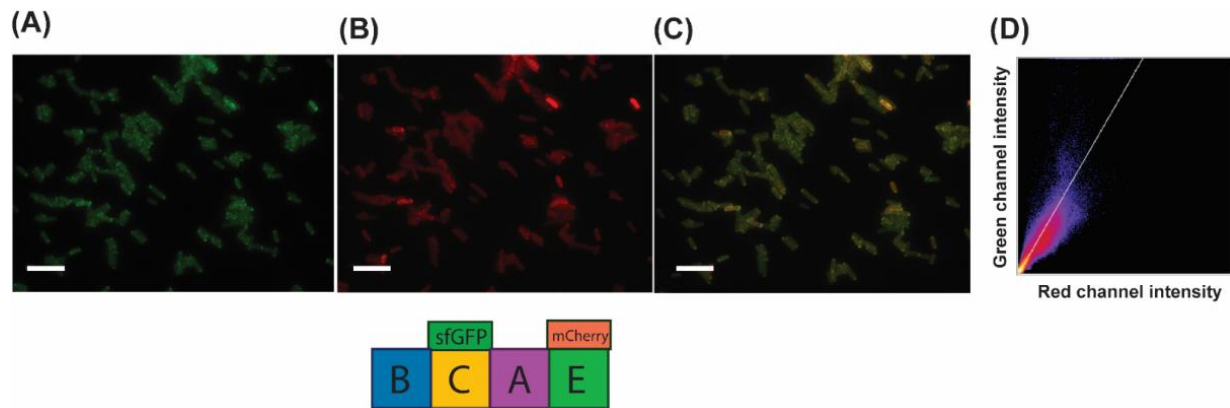


Figure 17 - (A-D) Fluorescence microscopy of cells expressing individual subunits PgsA, C, E, and B, respectively, each with sfGFP at the C-terminus. Variants of PgsB are (E) without signal peptide ( $PgsB\Delta 21$ ) and (F) and with only the signal peptide (ssPgsB). (G) sfGFP alone as cytoplasmic expression control. Each image represents the blind deconvolution of each captured z-stack. Side images represent orthogonal sections of the z-stack. Scale bar = 10  $\mu$ m.

To determine that all components of PGS are directed and co-localized to the *E. coli* cell membrane, we created two-fluorophore *pgs* operon constructs. All express PgsC fused to sfGFP and a second component (PgsB, A, or E) tagged with mCherry – giving PgsBrCgAE, PgsBCgArE,

and PgsBCgAEr (where r = red/mCherry and g = green/sfGFP). For the PgsBCgAEr, it is evident that both proteins colocalize since we found high correlation between the green and red fluorescence signals (Figure 18). This is indicative that the proteins are correctly expressed in this heterologous host. However, for the other constructs (BrCgAE and BCgAr) we were unable to detect both fluorescent signals simultaneously, even after extensive attempts to optimize induction. We found that insertion of a fluorophore in the operon structure had a strong polarity effect on downstream genes.



*Figure 18 - Fluorescence microscopy of cells expressing pgsBCgAEr operon, where the PgsC subunit is linked to sfGFP/green and PgsE to mCherry/red, both at the C-terminal. (A) GFP channel. (B) Red channel. (C) Overlay of both channels. (D) Fluorescence intensity of colocalized pixels from the green and red channels. Scale bar = 10  $\mu$ m.*

During the microscopy experiments we had to be very careful about the conditions used during expression and visualization. Cell morphology, and consequently protein localization, could drastically change if induction levels, temperature, and length of incubation were not adequate. Figure 19 shows an example of how these changes could occur. PgsB-sfGFP at high induction still presented a clear pattern of localization to the membrane. However, the cells were swollen and

elongated, with possible problems in cell division. On the other hand, PgsB $\Delta$ 21 presented foci of inclusion bodies, which are not adequate for this type of microscopy analysis. Lowering inducer concentration decreased the impact on cell morphology but resulted in much lower fluorescence and required longer exposure (that could photobleach the samples).

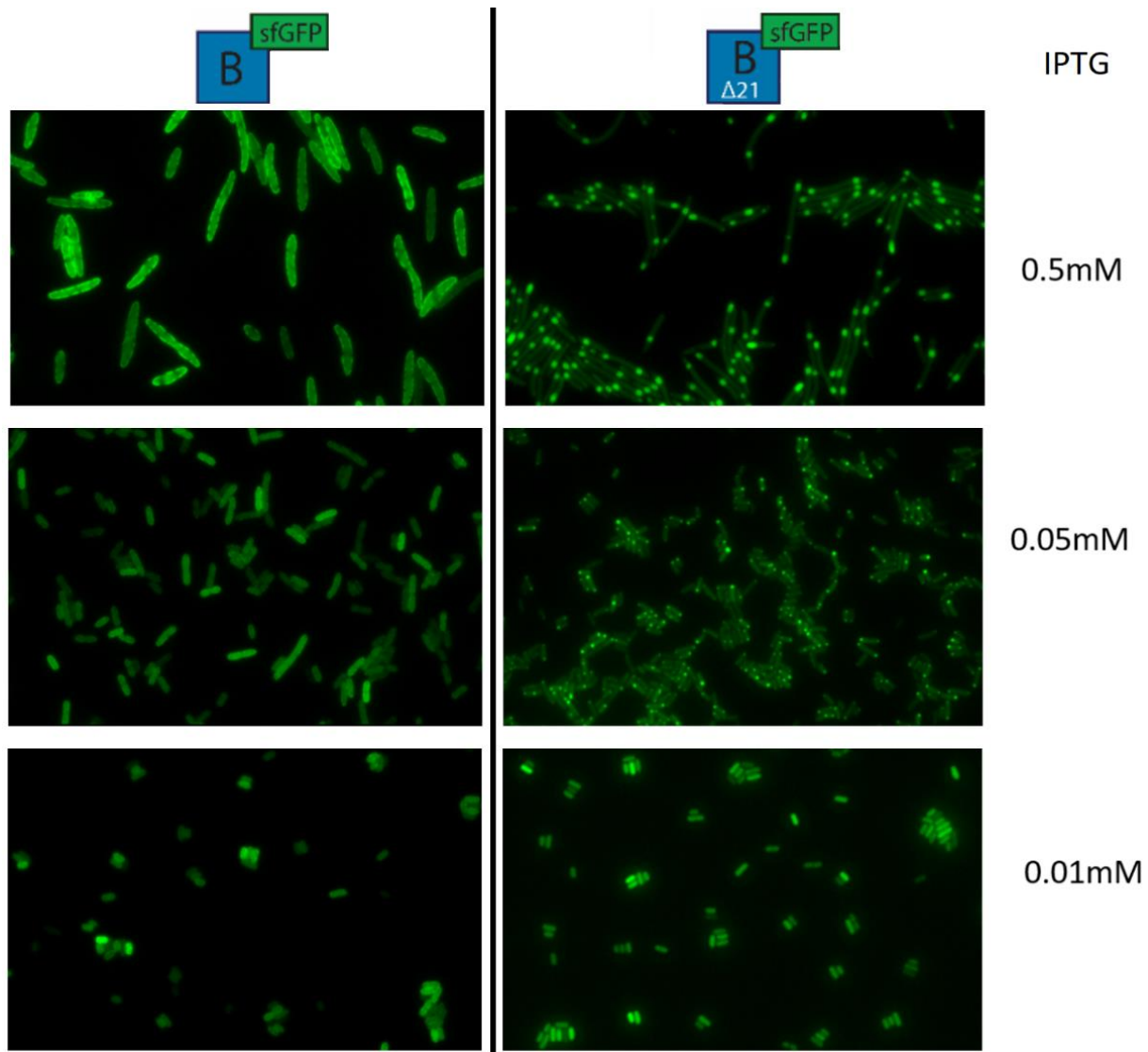


Figure 19 –Expression of PgsB and PgsB $\Delta$ 21 tagged with sfGFP at different induction levels of IPTG.

Observing under the microscope samples of *E. coli* MGΔΔ expressing PgsBCAE and producing PGA (Figure 20), we can confirm similar abnormalities in the cells. Additionally, at higher induction we observe a large number of lysed cells, which could come from either membrane stress by accumulation of high amount of PGS complexes or the accumulation of PGA intracellularly.

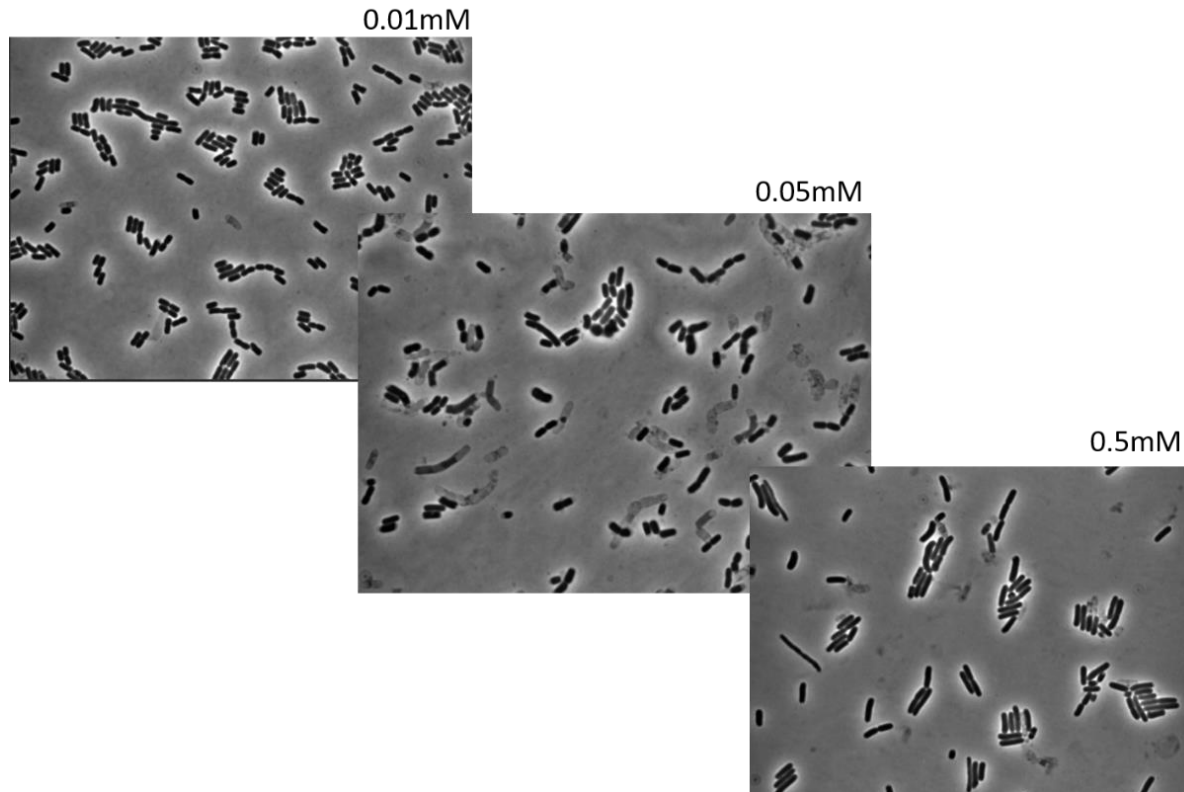


Figure 20 – Cell physiology of PgsBCAE at different induction levels of IPTG.

### 3.3.4 Topology of PGA synthetase subunits

Having confirmed that all four components of PGS localize to the membrane and that at least some of them co-localize, we wanted to determine the topology of each the polypeptide. The bioinformatic predictions summarized in Figure 15 indicate no clear consensus, likely due to the

fact that each method uses a different training set. Therefore, we want to experimentally determine the orientation of the different subunits in the inner membrane. For this, our reporters of choice were alkaline phosphatase (PhoA) and GFPuv as C-terminal fusions. PhoA is an enzyme that only folds correctly and presents activity if exported to the periplasm of *E. coli*, where disulfide bonds can be formed. In the presence of a specific substrate such as 5-bromo-4-chloro-3-indolyl phosphate (X-Pho), colonies expression PhoA in the periplasm develop a blue color, while colonies whose enzyme is expressed in the cytoplasm remains white (Jiménez-Guerrero et al. 2013). Conversely, GFPuv only fluoresces in the cytoplasm since the oxidizing environment in the periplasm promotes the formation of disulfide bonds between C49 and C71, which causes misfolding, impeding chromophore maturation (Dammeyer and Tinnefeld 2012).

Based on the predictions summarized in Figure 15, we expect only PgsC to have multiple transmembrane domains, with both cytoplasmic and periplasmic segments. Each of the other subunits are expected to wholly localized to either the cytoplasmic or periplasmic side of the inner membrane. We created PhoA fusions to each full-length PGS component and found that only PgsB did not develop a blue color, indicating that its C-terminus is in the cytoplasm (Figure 21A). All other components (PgsA, C, and E) developed a strong blue color signal suggesting their C-termini are periplasmically localized. For further analysis of PgsC, we created specific truncation (indicated by black arrows in Figure 2 and numbered subscripts in Figure 6) and fused them to PhoA. Figure 21A shows that only peptide 1–73 has a negative X-Pho signal, indicating that segments between 40 and 100 of PgsC are within the cytoplasm. All other truncations present as PhoA<sup>+</sup>, indicating periplasmic localization.

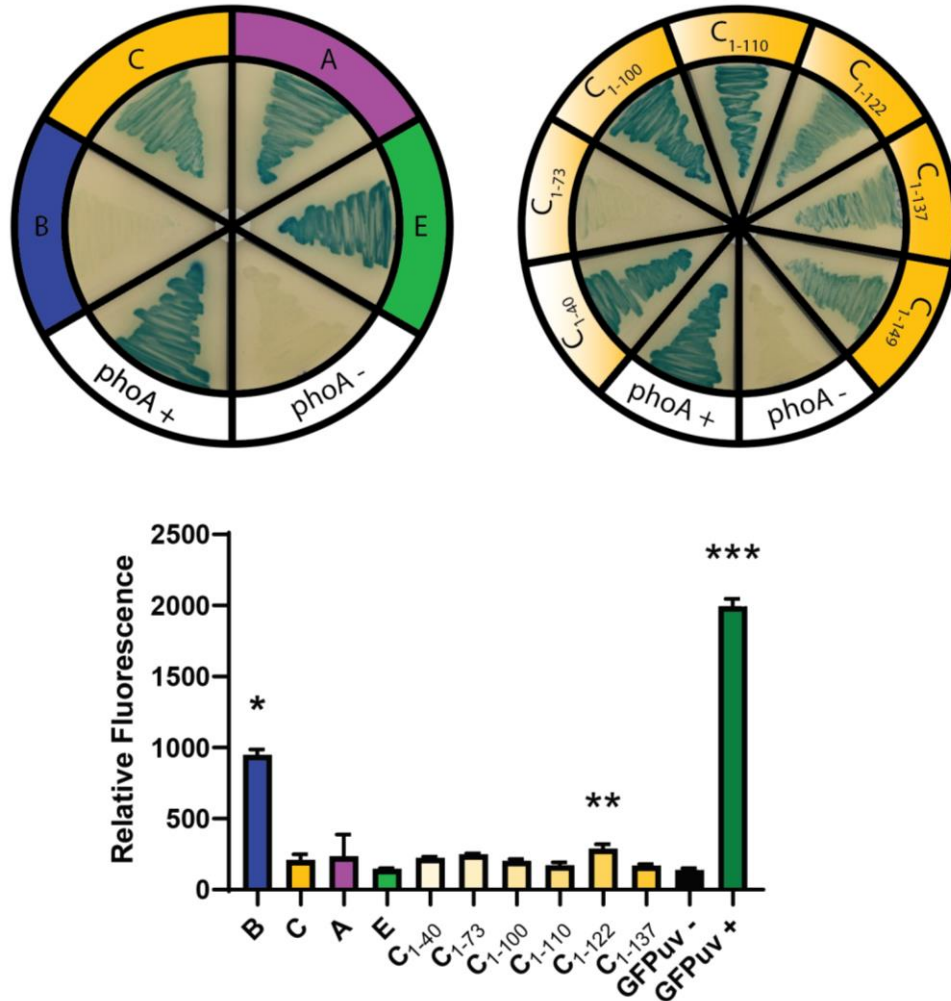


Figure 21 - (A) LB+X-Pho plates after induction with IPTG. Each section is an *E. coli* MGΔΔ strain expressing a full-length PGS subunit with a PhoA fusion at its C-terminus. At the bottom there is a positive and negative control for PhoA activity. Truncated versions of PgsC were also assayed by the same method. (B) Relative fluorescence (RFU/OD<sub>600</sub>) of *E. coli* MGΔΔ strains expressing each full-length subunit with GFPuv fused at its C-terminus. Negative and positive controls constituted of cells expressing GFPuv in the periplasm and cytoplasm, respectively. Error bars indicate standard deviation of triplicate experiments. Asterisks indicate samples statistically different from negative control ( $p < 0.05$ ).

To further confirm localization, we used the GFPuv fusions. Specifically, constructs that are positive for PhoA should be negative for fluorescence. In Figure 21B, PgsB presented a high

signal, corroborating the previous result that its C-terminus is in the cytoplasm. Since GFPuv fusions to full-length PgsC, PgsA, and PgsE subunits emit fluorescence that is not statistically different from the negative control (GFPuv<sup>-</sup>), we conclude that all these components terminate in the periplasmic space. While fully-folded and active GFPuv can be translocated to the periplasm by the Tat pathway (Drew et al. 2002), it is most likely that these subunits use the Sec-pathway, in which translocation is concurrent with translation. We expected, based on PhoA activity data, that PgsC fragment 1-73 would present a high fluorescence signal. However, only fragment 1-122 had fluorescence statistically different from the negative control, albeit much lower when compared the positive control (GFPuv<sup>+</sup>). Thus, the GFPuv data are not very conclusive about the topology of PgsC.

Taking the PhoA and GFPuv results together, we can construct a consensus schematic of these proteins in the inner membrane of *E. coli* (Figure 22). The results for PgsB are the most conclusive, having a very distinct signal for its presence in the cytoplasm. The predicted signal peptide from amino acids 1-21 does not direct the protein to the periplasm but rather to the cytoplasmic side of the inner membrane. Based on homology predictions (Sup. Fig. 2) and the proposed reaction mechanism (M. Ashiuchi and Misono 2002), this subunit has access to the cytoplasmic glutamate and nucleotide pools necessary for reaction. Similarly, results were quite conclusive for PgsA and PgsE, both of which are present largely in the periplasm. Discounting the GFPuv results for PgsC, where the signals are very weak, and using only results from PhoA activity, we conclude that it has at least two (and at most three) transmembrane regions with the bulk of the protein being in the periplasm.

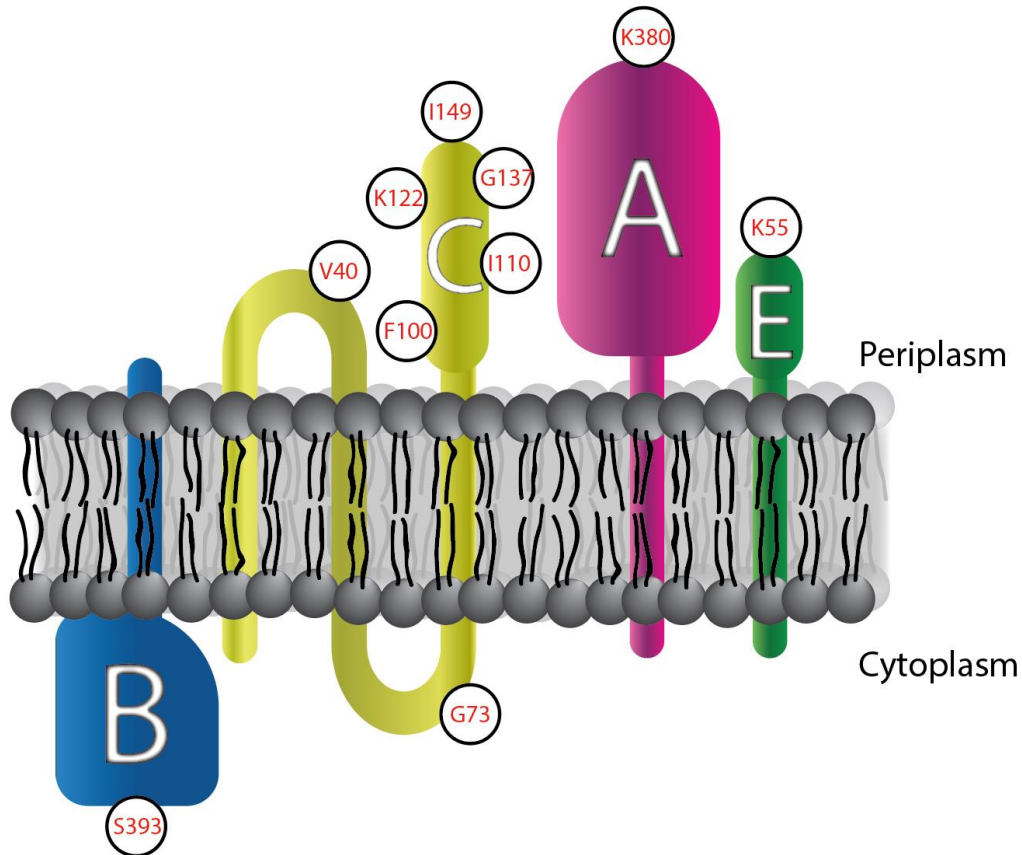


Figure 22 - Schematic representation of PgsBCAE localization at cell membrane. White circles indicate the amino acid location where reporter fusions were added.

### 3.4 Chapter conclusions

After successfully expressing the PgsBCAE membrane enzyme in *E. coli*, the difference in membrane structure between *B. subtilis* and *E. coli* motivated us to further investigate if the enzyme had the correct localization in the heterologous host. Bioinformatic analysis of the protein sequence provided insights into some basic structural properties. PgsB presented similarities with other amide ligases, and a putative ATP interaction site. The homology model constructed based on FolC even presented a channel for substrate entrance.

On the analytical side, correct expression of each subunit was verified by SDS-PAGE and Western blot. All presented the expected molecular weight, except for PgsC which was not detected. We presume that the intricate transmembrane pattern of PgsC prevents proper isolation of the protein in membrane fraction or access to the His-tag.

We also observed that the tagged enzyme subunits are correctly directed to the inner cell membrane by fluorescent microscopy, providing a clear reporter pattern across the cell membrane. We could also show for the first time the orientation of the N- and C- termini of the different components across the membrane. These results will help us further understand the role of each subunit in the complex and aid in future engineering efforts.

## Chapter 4: Conclusions and future work

---

### 4.1 General conclusions

In this study we successfully expressed the poly- $\gamma$ -glutamate synthetase (PGS) membrane enzyme in a heterologous host (*Escherichia coli*). This enzyme is responsible for the polymerization and secretion of poly- $\gamma$ -glutamate (PGA), an anionic polymer with unique bonds between the amino acid residues at the  $\gamma$ -carboxyl groups.

Even though the Gram-negative membrane structure of *E. coli* differs from the Gram-positive *B. subtilis* that naturally produces PGA, we could recover and detect the polymer from the *E. coli* culture supernatant, showing that the enzymatic complex was fully functional. Even though production was low due to the small scale of experiments, achieving 13 mg/L of PGA, the polymer presented a high molecular weight and minimal degradation due to the absence of hydrolytic enzymes in *E. coli*.

We also developed a fast semi-quantitative method to detect PGA: a dot blot with methylene blue staining. Positively charged nylon membranes were spotted with the culture supernatant (eliminating the need for a purification step, needed for other PGA detection methods) and the presence of PGA was detected with methylene blue staining.

The difference in membrane structure between *B. subtilis* and *E. coli* also motivated us to investigate if the enzyme had the correct localization in the heterologous host. Not only did we

observe that the tagged enzyme subunits are correctly directed to the inner cell membrane by microscopy and fluorescent reporters, but we could also demonstrated for the first time the orientation of the N- and C- termini of the different components across the membrane. Truncated versions of PgsB and PgsC also gave additional support to the structural traits predicted during bioinformatic analysis of the sequences. These results will help us further understand the role of each subunit in the PGS complex and aid in future engineering efforts.

We brought the findings accomplished with this dissertation to scientific events as oral presentations and posters, and part of the results were used to compose the article published at *Metabolic Engineering Communications*:

Motta Nascimento, Bruno; and Nair, Nikhil U. 2020. “Characterization of a membrane enzymatic complex for heterologous production of poly- $\gamma$ -glutamate in *E. coli*”. *Metabolic Engineering Communications* 11, e00144. <<https://doi.org/10.1016/j.mec.2020.e00144>>

## 4.2 Future directions

Finding of this work could foster some additional research in the future, that can be divided in these main areas:

- Enhance PGA production:

As discussed in previous chapters, the PGA polymer is a valuable product with industrial applications. We have successfully cloned and expressed the *B. subtilis* PGS genes in *E. coli* and produced a PGA polymer with high molecular weight. *B. subtilis* cultures have the disadvantage of also producing hydrolases that degrade PGA and less stringent control of PGS

expression. The heterologous system allows more control during gene expression and polymer synthesis. Further studies in bioprocessing could optimize the culture conditions for our *E. coli* strain (MG $\Delta\Delta$  with *pgsBCAE*) to produce higher titers of this valuable product.

- Further characterization of PGS:

In Chapter 3 we initiated the characterization of PGS subunits. These studies could move forward by creating additional versions of what was presented in our work (more sensitive reporters, better microscopy resolution) or dwelling in new analysis (co-localization/interaction of the subunits by FRET analysis). Topological analysis with PhoA/GFPuv could use other truncated versions of subunits to bring an even clearer picture of their membrane organization. The availability of more genetic engineering tools for *Bacillus* species now would allow similar studies in the original host as well.

- Structural biology studies:

So far there is limited information regarding the 3-dimensional structure of PGS due to difficulties in isolating a stable version of the whole complex and/or its subunits in their natural environment, the cell membrane. This is not surprising. Even though membrane proteins represent a substantial portion of total cell protein, they are extremely underrepresented in structural databases, with less than 2% of all resolved structures (Dörr et al. 2016). Recovery of a stable PGS in the membrane for X-ray crystallography or electron microscopy would require extensive studies with the use of different detergents, protein scaffolds, or nanodiscs. Recent developments in SMALPs co-polymers for structural biology also appear promising to this line of work.

- Identification of relevant residues for substrate binding and enzymatic activity:

Isolation a stable PGS could also help to develop an *in vitro* assay to elucidate in more detail the reacting mechanism of the enzyme. As we have observed during sequence analysis, PgsB has some conserved ATP-binding sites, which presumably are essential for activity. Identification of other relevant residues that interact with L- and D-glutamate are essential for unveiling more into this enzyme characteristics. Creating a mutant library of PgsB, we could rationally alter those interactions and observe the effects. This line of work is highly dependent on developments discussed in the previous bullet points, because rational protein evolution requires a lot of previous structural information. Having an insight into this substrate/enzyme interaction could allow us to further push into constructing mutant library to alter PGS substrate specificity. As discussed in Chapter 1, other polyamino acids have very desirable industrial applications. Nevertheless, they can only be produced by chemical synthesis. Altering substrate specificity of PGS to accept other amino acids (aspartate, lysine, arginine, or even non-natural amino acids) could make available a new biosynthetic process for these desired polymers.

# Supplemental material

CLUSTAL O (1.2.4) multiple sequence alignment of PgsB with other enzymes identified during homology prediction

```

B_anthraxis_P19580      -----MKNIKIVRILKH-----DEAIRIE
B_licheniformCGMCC2876-----
B_licheniformis_WBL-3 -----
B_amyloliquefaciensLL3-----
B_subtilis_chungkookja-----
B_subtilis_NX-2        -----
B_subtilis_IF03336     -----
B_subtilis_ATCC_6633   -----
B_subtilis_HSF1410    -----
B_subtilis_GXA-28     -----
B_licheniformis_NK-03 -----
E_coli_folC            -----
B_subtilis_folC       -----
E_coli_murC            MNTQQQLAKLRSIVPEM-RRVRHIHFVG--IG--GAGMGGIAEVLN-----EGYQIS
E_coli_murD            -----MA-D-YQGKNVVIIG--LG--LTGLSCVDFFLARGVTPRVM DTRMTPP
E_coli_murE            MA---DRNLRDLLAPWVPDAPSRALREMTLDSRVAAAGD--LFVA-----VVGHQAD
E_coli_murF            MISVTLSQLTDI LNGEL-QGADITLDAVTTDTRKLT PGC--LFVA-----LKGERFD
  
```

```

B_anthraxis_P19580      --HRISELYSDEFGVVYAGNHLIFN WYQRLYLSRNI-LISKKSRSRKGLIQMIFIIGICT
B_licheniformCGMCC2876-----MWVMLLAC
B_licheniformis_WBL-3 -----MWVMLLAC
B_amyloliquefaciensLL3-----MWLLIIAC
B_subtilis_chungkookja-----MGWLLIIAC
B_subtilis_NX-2        -----MWLLIIAC
B_subtilis_IF03336     -----MWLLIIAC
B_subtilis_ATCC_6633   -----MWLLIIAC
B_subtilis_HSF1410    -----MWLLIIAC
B_subtilis_GXA-28     -----MWLLIIAC
B_licheniformis_NK-03 -----MWLLIIAC
E_coli_folC            -----MIKRTPPQAAS-----PLASWLSYLENLH SKTIDLGLER
B_subtilis_folC       -----MFTAYQ-----DARSWI---HGRLKFGVKPGLGR
E_coli_murC            GSDLAPNP--VTQQLMNLGATIYFNHRPENVRDASVVVVSSAISADNPEIVAAHEARIPV
E_coli_murD            GLDKLPEA--VERHTGSL-----NDEWLMAADLIVASPGIALAHPSLSAAADAGIEI
E_coli_murE            GRRYIPQA--IAQGVAAI-----IAEAKDEATDGEIREMHGVPVIY
E_coli_murF            AHDFADQA--KAGGAGAL-----LVSRPLDI-----DLPQLI
  
```

```

B_anthraxis_P19580      V--FLIIYGIWEQRCHQKRLNSIPRVNNGIRGKSTVTRLITGVVQEAKYKTVGKTTGT
B_licheniformCGMCC2876V--IVVGIGIYEKRRHQQNIDALPVRVNINGIRGKSTVTRLTTGILIEAGYKTVGKTTGT
B_licheniformis_WBL-3 V--IVVGIGIYEKRRHQQNIDALPVRVNINGIRGKSTVTRLTTGILIEAGYKTVGKTTGT
B_amyloliquefaciensLL3A--AVLIIGIIEKRRHQKNIDALPVRVNINGIRGKSTVTRLTTGILMEAGYKTVGKTTGT
B_subtilis_chungkookjaA--VILVIGILEKRRHQKNIDALPVRVNINGIRGKSTVTRLTTGILIEAGYKTVGKTTGT
B_subtilis_NX-2        A--VILVIGILEKRRHQKNIDALPVRVNINGIRGKSTVTRLTTGILIEAGYKTVGKTTGT
B_subtilis_IF03336     A--VILVIGILEKRRHQKNIDALPVRVNINGIRGKSTVTRLTTGILIEAGYKTVGKTTGT
B_subtilis_ATCC_6633   A--VILVIGILEKRRHQKNIDALPVRVNINGIRGKSTVTRLTTGILIEAGYKTVGKTTGT
B_subtilis_HSF1410    A--VILVIGILEKRRHQKNIDALPVRVNINGIRGKSTVTRLTTGILIEAGYKTVGKTTGT
B_subtilis_GXA-28     A--VILVIGILEKRRHQKNIDALPVRVNINGIRGKSTVTRLTTGILIEAGYKTVGKTTGT
B_licheniformis_NK-03 A--VILVIGILEKRRHQKNIDALPVRVNINGIRGKSTVTRLTTGILIEAGYKTVGKTTGT
E_coli_folC            VSLVAARLGV-----LKPAPFVFTVAGTNGKGTTCRTL ESILMAAGYKVG VYSSPH
  
```

**B\_subtilis\_folC** MKQLMARLGH-----PEKKIRAFHVAGTNGKGS TVAFIRSMLEAGYTVGTFSTSPY  
**E\_coli\_murC** IRRRA-----E-MLAELMRFRHGIAIAGTHGKTT TTAMVSSIYAEAGLDPT---FVN  
**E\_coli\_murD** VGDI-----E-LFCREA-QAPIVAITGSNGKST VTTLVGEMAKAAGVNVG-----  
**E\_coli\_murE** LSQNLNRLSALAGR-FYHEPSDNLRLVGVGTGNKTT TTQLLAQWSQLLGEPSAVMGTVG  
**E\_coli\_murF** VKDTRLAFGELA---AWVRQQVPARVVALTGSSGKTS VKEMTAAIILSQCGNTLYTAGNLN  
. : \* \*\* :.

**B\_anthraxis\_P19580** SARMIYWFTD---EEQPIK-----RRKEGPNIGEQRV--VK-----EA  
**B\_licheniformCGMCC2876** DARMIYWDTP---EEKPIK-----RKPQGNIGEQQEV--MK-----ET  
**B\_licheniformis\_WBL-3** DARMIYWDTP---EEKPIK-----RKPQGNIGEQQEV--MK-----ET  
**B\_amyloliquefaciensLL3** DARMIYWDTP---EEKPIK-----RKPQGNIGEQQEV--MK-----ET  
**B\_subtilis\_chungkookja** DARMIYWDTP---EEKPIK-----RKPQGNIGEQQEV--MR-----ET  
**B\_subtilis\_NX-2** DARMIYWDTP---EEKPIK-----RKPQGNIGEQQEV--MR-----ET  
**B\_subtilis\_IF03336** DARMIYWDTP---EEKPIK-----RKPQGPSIGEQQEV--MR-----ET  
**B\_subtilis\_ATCC\_6633** DARMIYWDTP---EEKPIK-----RKPQGNIGEQQEV--MK-----ET  
**B\_subtilis\_HSF1410** DARMIYWDTP---EEKPIK-----RKPQGNIGEQQEV--MR-----ET  
**B\_subtilis\_GXA-28** DARMIYWDTP---EEKPIK-----RKPQGNIGEQQEV--MR-----ET  
**B\_licheniformis\_NK-03** DARMIYWDTP---EEKPIK-----RKPQGNIGEQQEV--MR-----ET  
**E\_coli\_folC** ---LVRYTERVRVQOQELPESAHASFAEIESARGDISLT-----YFEY-GTLSALWLF  
**B\_subtilis\_folC** ---ITFNERISVNGIPIISDEEWALVNQMKPHEALDQTEYGPTEFEIMTACAFLYFA  
**E\_coli\_murC** -----GGL--VKA-----AGVHA-----RLGHGR-----YLIA  
**E\_coli\_murD** -----VGG-----NIGLPA-----LMLL  
**E\_coli\_murE** -----NGL--LGKVIPTENTGS-----AVDVQH-----ELAGL  
**E\_coli\_murF** -----NDI-----G-----VPM-----TLRL

**B\_anthraxis\_P19580** ADLEAEALICE CMAVQPDYQIIFQNKMIQANVGIVNVLE DHMD VMGPTLDEVAEAF TA-  
**B\_licheniformCGMCC2876** VERGANAVVSE CMAVNPDYQIIFQEELLQANIGVIVNVLE DHMD VMGPTLDEIAEAF TA-  
**B\_licheniformis\_WBL-3** VERGANAIVSE CMAVNPDYQIIFQEELLQANIGVIVNVLE DHMD VMGPTLDEIAEAF TA-  
**B\_amyloliquefaciensLL3** VERGANAIVSE CMAVNPDYQIIFQEELLQANIGVIVNVLE DHMD VMGPTLDEIAEAF TA-  
**B\_subtilis\_chungkookja** VERGANAIVSE CMAVNPDYQIIFQEELLQANIGVIVNVLE DHMD VMGPTLDEIAEAF TA-  
**B\_subtilis\_NX-2** VDRGANAIVSE CMAVNPDYQIIFQEELLQANIGVIVNVLE DHMD VMGPTLDEIAEAF TA-  
**B\_subtilis\_IF03336** VERGANAIVSE CMAVNPDYQIIFQEELLQANIGVIVNVLE DHMD VMGPTLDEIAEAF TA-  
**B\_subtilis\_ATCC\_6633** VERGANAIVSE CMAVNPDYQIIFQEELLQANIGVIVNVLE DHMD VMGPTLDEIAEAF TA-  
**B\_subtilis\_HSF1410** VERGANAIVSE CMAVNPDYQIIFQEELLQANIGVIVNVLE DHMD VMGPTLDEIAEAF TA-  
**B\_subtilis\_GXA-28** VERGANAIVSE CMAVNPDYQIIFQEELLQANIGVIVNVLE DHMD VMGPTLDEIAEAF TA-  
**B\_licheniformis\_NK-03** VERGANAIVSE CMAVNPDYQIIFQEELLQANIGVIVNVLE DHMD VMGPTLDEIAEAF TA-  
**E\_coli\_folC** KQAQLDVVILE -VGL---GGRLDATNIVDADVAVVTSIALDHT DWLGPDRSIGREKAGI  
**B\_subtilis\_folC** EFHKVDFVIFE -TGL---GGRFDSTNVVEPLLVITSIGHDHM NILGNTIEE IAGEKAGI  
**E\_coli\_murC** EADES-----ASFLHLQPMVAIVTNI EADHMD TYQGDFENLQKTFINF  
**E\_coli\_murD** -DDECELYVLE -LSS----FQLETTSSLQAVAATILNVTE DHMD RYPFGLQYRAAK---  
**E\_coli\_murE** VDQGATFCAME ---VSSHGLVQHRVAALKFAASVFTNLSR DHLD -YHGDMHYEAAKWLL  
**E\_coli\_murF** T-PEYDYAVIE -LGANHQGEI IAWTVSLTRPEAALVNLA AAHLE -GFGSLAGVAKAKGEI  
. . : \* :

**B\_anthraxis\_P19580** --TIPYNGHLVTIE---SEYLDYFKEVAEERN-----TKVIVADNS-----  
**B\_licheniformCGMCC2876** --TIPYNGHLVITD---SEYDFFKQIAKERN-----TKVIVADNS-----  
**B\_licheniformis\_WBL-3** --TIPYNGHLVITD---SEYDFFKQIAKERN-----TKVIVADNS-----  
**B\_amyloliquefaciensLL3** --TIPYNGHLVITD---SEYDFFKEKAAERN-----TEVIADNS-----  
**B\_subtilis\_chungkookja** --TIPYNGHLVITD---SEYTEFFKQKAKERN-----TKVIIADNS-----  
**B\_subtilis\_NX-2** --TIPYNGHLVITD---SEYTEFFKQKAKERN-----TKVIIADNS-----  
**B\_subtilis\_IF03336** --TIPYNGHLVITD---SEYTEFFKQKAKERN-----TKVIIADNS-----  
**B\_subtilis\_ATCC\_6633** --TIPYNGHLVITD---SEYTEFFKQKAKERN-----TKVIIADNS-----  
**B\_subtilis\_HSF1410** --TIPYNGHLVITD---SEYTEFFKQKAKERN-----TKVIIADNS-----  
**B\_subtilis\_GXA-28** --TIPYNGHLVITD---SEYTEFFKQKAKERN-----TKVIIADNS-----  
**B\_licheniformis\_NK-03** --TIPYNGHLVITD---SEYTEFFKQKAKERN-----TKVIIADNS-----  
**E\_coli\_folC** FRS----EKPAIVGE--PEMPSTIADVAQEKGALLQR---RGVEWNYS-----

B\_subtilis\_folC IKE----GIPIVTAVTQPEALQVIRHEAERHAAPFQSLHDACVIFNEEA-----  
E\_coli\_murC LHNLPFYGRAVMCV-DDPVIRELLPRVGRQTT-----TYGFSEDA---DVRVEDYQ  
E\_coli\_murD ---LRIYENAKVCV-VNADDALTMPIRGADER-----CVSFG-----VNMGDYH  
E\_coli\_murE YS-AHHCQGAIINA-DDEVGRWLAKLPDAVA-----VSMEDHINPNCHGRWLKATDVN  
E\_coli\_murF FSGLPENGIAMNA-DNNDWLNWQSVIGSRKV-----WRFSPNAANSDFATNIIH

B\_anthraxis\_P19580 -----RISEEF LRKF DYMVFPDNASLALAV-----AEALGIDEETA FRG  
B\_licheniformCGMCC2876-----KITDEYLRQFEYMVFPDNASLALGV-----AQALGIDEETA FRG  
B\_licheniformis\_WBL-3 -----KITDEYLRQFEYMVFPDNASLALGV-----AQALGIDEETA FRG  
B\_amyloliquefaciensLL3-----KITDEYLRKFEYMVFPDNASLALGV-----AQALGIDEETA FRG  
B\_subtilis\_chungkookja-----KITDEYLRNFEYMVFPDNASLALGV-----AQALGIDEETA FRG  
B\_subtilis\_NX-2 -----KITDEYLRKFEYMVFPDNASLALGV-----AQALGIDEETA FRG  
B\_subtilis\_IF03336 -----KITDEYLRKFEYMVFPDNASLALGV-----AQALGIDEETA FRG  
B\_subtilis\_ATCC\_6633 -----KITDEYLRKFEYMVFPDNASLALGV-----AQALGIDEETA FRG  
B\_subtilis\_HSF1410 -----KITDEYLRKFEYMVFPDNASLALGV-----AQALGIDEETA FRG  
B\_subtilis\_GXA-28 -----KITDEYLRKFEYMVFPDNASLALGV-----AQALGIDEETA FRG  
B\_licheniformis\_NK-03 -----KITDEYLRKFEYMVFPDNASLALGV-----AQALGIDEETA FRG  
E\_coli\_folC ---VTDHDWAFSDAHGTLENLPLPLVPPQNA--TALAAL-----RASGLEVSENAIRDG  
B\_subtilis\_folC --LPAGEQFSFKTEEKCYEDIRTSLIGTHQRQNAALSILAAEWLNKENIAHISDEALRSG  
E\_coli\_murC QIGPQGHFTL-LRQDKEPMRVTLNAPGRHNALNAAA AVAV-----ATEEGIDDEAILRA  
E\_coli\_murD LNHQQGETWLRVKGEKVLNVKEMKLSGQHNYTNALALAL-----ADAAGLPRASSLKA  
E\_coli\_murE YHDSG--ATIRFSSSWGDEIESRLMGAFNVSNLLALAT-----LLALGYPLADLLKT  
E\_coli\_murF VTSHG--TEFTLQTPTGSVDVLLPLPGRHNIANALAAAAAL-----SMSVGATLDAIKAG

:

B\_anthraxis\_P19580 MLNAPDPGAMRITRF-----ADQSKPAFFVNGFAANDPSSTLRI-----WER  
B\_licheniformCGMCC2876MLNAPPDPGAMRILPL-----MNAKNPGHFVNGFAANDAAS TLNI-----WKR  
B\_licheniformis\_WBL-3 MLNAPPDPGAMRILPL-----MNAKNPGHFVNGFAANDAAS TLNI-----WKR  
B\_amyloliquefaciensLL3MLNAPPDPGAMRILPL-----LSTKEPGHFVNGFAANDAS TLNI-----WKR  
B\_subtilis\_chungkookjaMLNAPPDPGAMRILPL-----ISPSEPGHFVNGFAANDAS TLNI-----WKR  
B\_subtilis\_NX-2 MLNAPPDPGAMRILPL-----ISPSEPGHFVNGFAANDAS TLNI-----WKR  
B\_subtilis\_IF03336 MLNAPPDPGAMRILPL-----ISPSEPGHFVNGFAANDAS TLNI-----WKR  
B\_subtilis\_ATCC\_6633 MLNAPPDPGAMRILPL-----ISPSEPGHFVNGFAANDAS TLNI-----WKR  
B\_subtilis\_HSF1410 MLNAPPDPGAMRILPL-----ISPSEPGHFVNGFAANDAS TLNI-----WKR  
B\_subtilis\_GXA-28 MLNAPPDPGAMRILPL-----ISPSEPGHFVNGFAANDAS TLNI-----WKR  
B\_licheniformis\_NK-03 MLNAPPDPGAMRILPL-----ISPSEPGHFVNGFAANDAS TLNI-----WKR  
E\_coli\_folC IA-SAILPGRFQIVSESPRVIFDV-----AHNPHAAEYLTGRMKALPKNGRVLA  
B\_subtilis\_folC LV-KAAWPGRLELVQEHPVYLDG-----AHNEEGVEKLAETMKQRFANSRISV  
E\_coli\_murC LESFQGTGRRFDLGEFPLEPVNGKSGTAMLVDDYGHHPTEVDATIKAA--RA-G--W-P  
E\_coli\_murD LTTFTGLPHRFVLEHNGV-----RWINDSKATN---VGSTE-AA--LN-G--LHV  
E\_coli\_murE AARLQPVCGRMEVFTA-----PGKPTVVV-DYAHTPDALEKALQ-----AARLHC  
E\_coli\_murF LANLKAVPGRLFPIQL-----AENQLLDDSYNANVGSMTAAVQVLAEMP-GYRVLV

:

B\_anthraxis\_P19580 ---VDDFGYSNLAPIVIMNCRPDRV-----DRT-EQFARDVLPYIKAEIVIAIG  
B\_licheniformCGMCC2876---VKEIGYPTDQPIVIMNCRDRV-----DRT-QQFADGVLPYIEASELVLIG  
B\_licheniformis\_WBL-3 ---VKEIGYPTDQPIVIMNCRDRV-----DRT-QQFAEDVLPYIEASELVLIG  
B\_amyloliquefaciensLL3---VKEIGYPTDEPIVIMNCRDRV-----DRT-IQFANDVLPYIKTELILIG  
B\_subtilis\_chungkookja---VKEIGYPTDDPIIIMNCRDRV-----DRT-QQFANDVLPYIEASELILIG  
B\_subtilis\_NX-2 ---VKEIGYPTDDPIIIMNCRDRV-----DRT-QQFANDVLPYIEASELILIG  
B\_subtilis\_IF03336 ---VKEIGYPTDDPIIIMNCRDRV-----DRT-QQFANDVLPYIEASELILIG  
B\_subtilis\_ATCC\_6633 ---VKEIGYPTDDPIIIMNCRDRV-----DRT-QQFANDVLPYIEASELILIG  
B\_subtilis\_HSF1410 ---VKEIGYPTDDPIIIMNCRDRV-----DRT-QQFANDVLPYIEASELILIG  
B\_subtilis\_GXA-28 ---VKEIGYPTDDPIIIMNCRDRV-----DRT-QQFANDVLPYIEASELILIG  
B\_licheniformis\_NK-03 ---VKEIGYPTDDPIIIMNCRDRV-----DRT-QQFANDVLPYIEASELILIG  
E\_coli\_folC -----VIGMLHKDIDIAGTLAWLKSVDVDD-----WYCAPL----

```

B_subtilis_folC      -----VFSALKDKPYQNMIKRLETIAHA-----IHFASF----
E_coli_murC          DKNL-----VMLFQPHR-----FTRTRDLYDDFANV-LTQ
E_coli_murD          DRTL-----HLLGGD-----GKSADFSPL----
E_coli_murE          AGK-----LWCVFGGGDRD-K-----GKR----PLMGAIAEFADV-AVV
E_coli_murF          VGDMAELGAES--EACHVQVGEAAKAAGID-RVLSVKGQSHAISTASGVGEHFADK-TAL

```

```

B_anthraxis_P19580  ETTAPITSAFEKGDIPQ-----EYWNLEGW---STSEIM---SRMRPY
B_licheniformisCGMCC2876ETTEPIVKAYEAGKIPAD-----KLFDFEHK---STEEIM---FMLKKN
B_licheniformis_WBL-3 ETTEPIVKAYEAGKIPAD-----KLFDFEHK---STEEIM---FMLKKN
B_amyloliquefaciensLL3ETTEPIVRAAYEEGKIPAD-----TLHDLEYK---STDEIM---DVLKTR
B_subtilis_chungkookjaETTEPIVKAYEEGKIPAD-----KLHDLEYK---STDEIM---ELLKKR
B_subtilis_NX-2      ETTEPIAKAYEEGKIPAD-----KLHDLEYK---STDEIM---ELLKKR
B_subtilis_IF03336   ETTEPIVKAYEEGKIPAD-----KLHDLEYK---STDEIM---ELLKKS
B_subtilis_ATCC_6633 ETTEPIVKAYEEGKIPAD-----KLHDLEYK---STEEIM---ELLKKR
B_subtilis_HSF1410  ETTEPIVKAYEEGKIPAD-----KLHDLEYK---STDEIM---ELLKKR
B_subtilis_GXA-28    ETTEPIVKAYEEGKIPAD-----KLHDLEYK---STDEIM---ELLKKR
B_licheniformis_NK-03 ETTEPIVKAYEEGKIPAD-----KLHDLEYK---STDEIM---ELLKKR
E_coli_folC          -----EGPRGATAEQLEHL--GNGKSFDSVAQ--AWDAAMAD-----
B_subtilis_folC      -----DFPRASLAKDLYDAS--E-----ISNK---SWSEDPDDVIKFIKESK
E_coli_murC          VDTLLMLEVYPAGEAIPGADSRSLCRTIRGRGKIDPILVPDPA-----RVAEMLAPV
E_coli_murD          -----ARY-----LNGDNVRLYCFGRDGAQ--LAALRPEVAEQTETMEQAMRLLAPR
E_coli_murE          TDDNPR-----TEEPRAIINDILAG---MLDAGYAKVMEGRAEA
E_coli_murF          ITRLKL-----LIAEQQVITILVKG---SRSAAMEEVVRLQEN

```

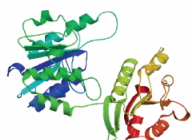
```

B_anthraxis_P19580  -----LKNRIVYGVGNIHGAAEPLIDMIMEEQIGKKQAKVI-----
B_licheniformisCGMCC2876-----LEGRVIYGVGNIHGAAEPLIEKIQDYKIKQLVS-----
B_licheniformis_WBL-3 -----LEGRVIYGVGNIHGAAEPLIEKIQDYKIKQLVS-----
B_amyloliquefaciensLL3 -----MQNRVIYGVGNIHGAAEPLIEKIQDYKIKQLVS-----
B_subtilis_chungkookja-----MHN RVIYGVGNIHGAAEPLIEKIHEYKVKQLV-----
B_subtilis_NX-2      -----MHN RVIYGVGNIHGAAEPLIEKIHEYKVKQLVS-----
B_subtilis_IF03336   -----MHN RVIYGVGNIHGAAEPLIEKIHEYKVKQLVS-----
B_subtilis_ATCC_6633 -----MHN RVIYGVGNIHGAAEPLIEKIHEYKVKQLVS-----
B_subtilis_HSF1410  -----MHN RVIYGVGNIHGAAEPLIEKIHEYKVKQLVS-----
B_subtilis_GXA-28    -----MHN RVIYGVGNIHGAAEPLIEKIHEYKVKQLVS-----
B_licheniformis_NK-03 -----MHN RVIYGVGNIHGAAEPLIEKIHEYKVKQLVS-----
E_coli_folC          -----AKAEDTVLVCGSFHTVAHVMEVIDARRS-----GGK-----
B_subtilis_folC      -----KGSNEIVLITGSLYFISDIRKRLK-----
E_coli_murC          -----LTGNDLILVQGA-----GNIGKIARSLAEIKLKPQTPEEEQHD
E_coli_murD          -----VQPGDMVLLSPACASLDQFK-NFEQRGNEFARLAKELG-----
E_coli_murE          VTCAVMQAKENDVVLVAGKGHEDYQIVGNQRLDYSDRVTVARLLGVIA-----
E_coli_murF          GTC-----

```

Sup. Fig. 1 - Multiple sequence alignment by CLUSTAL O of PgsB from Bacilli (black labels) and other poly-amino-acid synthetases (red labels). The putative sites of interaction with ATP are highlighted in yellow.

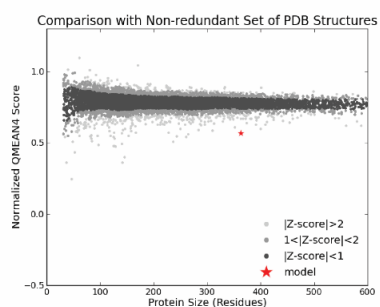
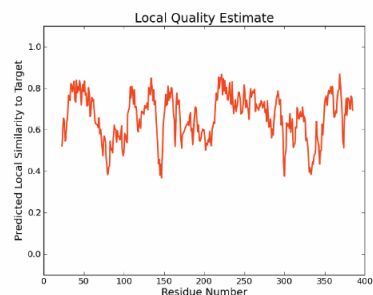
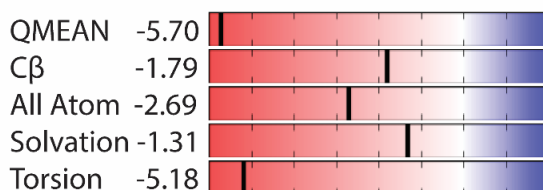
## PgsB



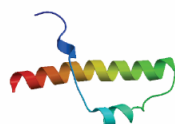
Homology model built with ProMod3 Version 1.0.2.

GMQE: 0.49  
QMEAN: -5.70

Template:	UDP-N-ACETYLMURAMOYLALANYL-D-GLUTAMYL-2,6-DIAMINOPIMELATE-D-ALANYL-D-ALANYL LIGASE
PDB:	1GG4
Coverage:	81%
Range:	23-385
Seq. similarity:	29%



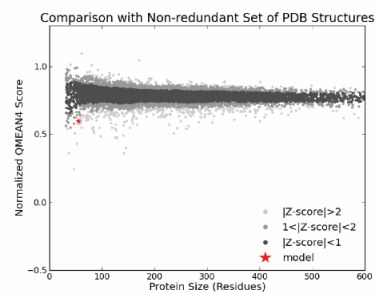
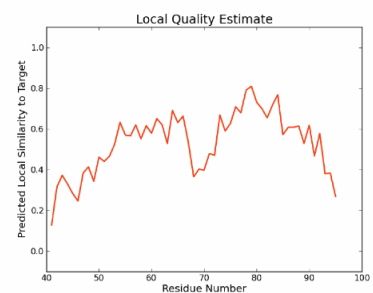
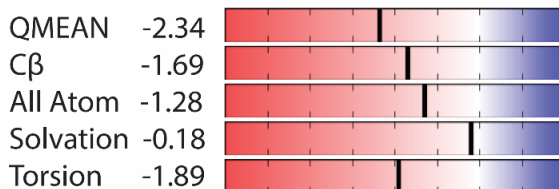
## PgsC



Homology model built with ProMod3 Version 1.0.2.

GMQE: 0.17  
QMEAN: -2.34

Template:	GlpG, rhomboid intramembrane serine protease
PDB:	2IRV
Coverage:	34%
Range:	41-95
Seq. similarity:	25%



Sup. Fig. 2 – Homology models for each PgsBCAE subunit obtained with SWISS-MODEL server (Schwede et al. 2003).

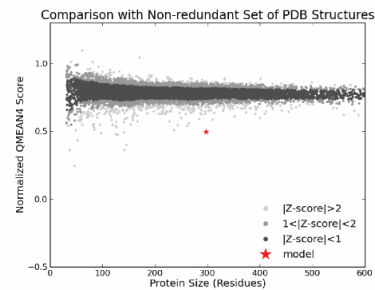
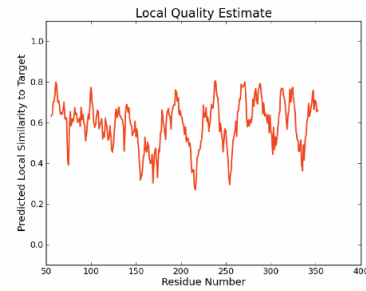
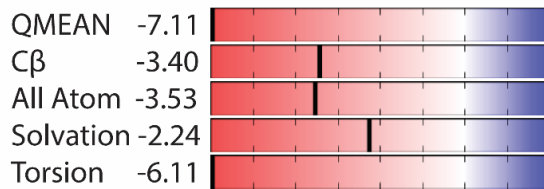
## PgsA



Homology model built with ProMod3 Version 1.0.2.

GMQE: 0.35  
QMEAN: -7.11

Template:	Exonuclease, putative
PDB:	4O24
Coverage:	69%
Range:	55-352
Seq. similarity:	27%



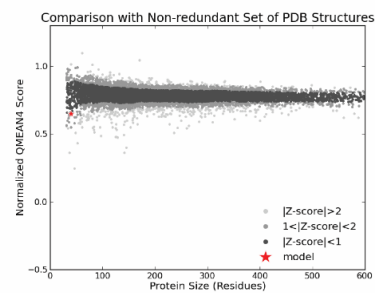
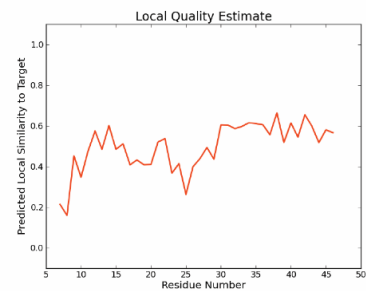
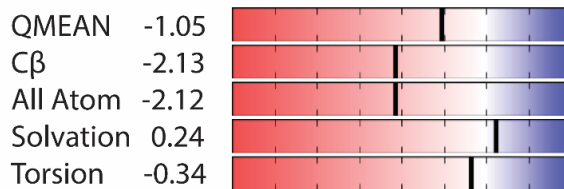
## PgsE



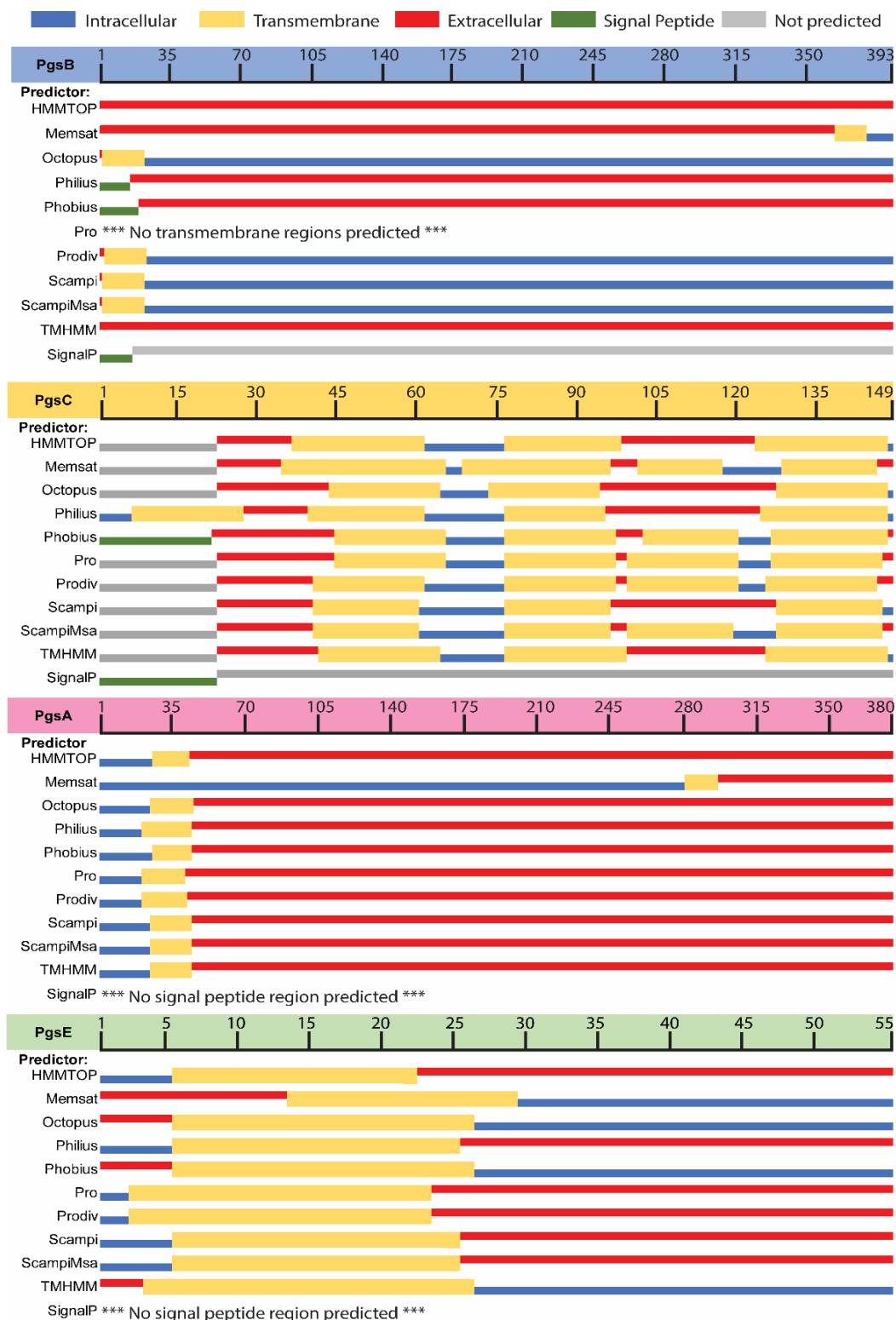
Homology model built with ProMod3 Version 1.0.2.

GMQE: 0.43  
QMEAN: -1.05

Template:	ATP synthase subunit b
PDB:	5T4Q
Coverage:	73%
Range:	7-46
Seq. similarity:	27%



Sup. Fig. 2 (cont.) – Homology models for each PgsBCAE subunit obtained with SWISS-MODEL server (Schwede et al. 2003).



Sup. Fig. 3 - Individual topology prediction by different server algorithms (HMMTOP, Memsat, Octopus, Philius, Phobius, Pro, Prodiv, Scampi-single, Scampi-msa, TMHMM, SignalP) (Dobson, Reményi, and Tuszányi 2015).

## Bibliography

---

- Ashiuchi, M., and H. Misono. 2002. "Biochemistry and Molecular Genetics of Poly- $\gamma$ -Glutamate Synthesis." *Applied Microbiology and Biotechnology* 59 (1): 9–14. <https://doi.org/10.1007/s00253-002-0984-x>.
- Ashiuchi, M, K Tani, K Soda, and H Misono. 1998. "Properties of Glutamate Racemase from *Bacillus Subtilis* IFO3336 Producing Poly-Gamma-Glutamate." *Journal of Biochemistry* 123 (6): 1156–63.
- Ashiuchi, Makoto. 2011. "Analytical Approaches to Poly- $\gamma$ -Glutamate: Quantification, Molecular Size Determination, and Stereochemistry Investigation." *Journal of Chromatography B: Analytical Technologies in the Biomedical and Life Sciences* 879 (29): 3096–3101. <https://doi.org/10.1016/j.jchromb.2011.03.029>.
- . 2013. "Microbial Production and Chemical Transformation of Poly- $\gamma$ -Glutamate." *Microbial Biotechnology* 6 (6): 664–74. <https://doi.org/10.1111/1751-7915.12072>.
- Ashiuchi, Makoto, Yuichi Hakumai, Sawami Nakayama, Haruna Higashiuchi, and Kosuke Shimada. 2018. "Engineering Antimicrobial Coating of Archaeal Poly- $\gamma$ -Glutamate-Based Materials Using Non-Covalent Crosslinkages." *Scientific Reports* 8 (4645): 1–10. <https://doi.org/10.1038/s41598-018-23017-x>.
- Ashiuchi, Makoto, Yuichi Hakumai, Shigeo Shibatani, Hirofumi Hakuba, Nogiho Oka, Hisato Kobayashi, and Keizo Yoneda. 2015. "Poly- $\gamma$ -Glutamate-Based Materials for Multiple

- Infection Prophylaxis Possessing Versatile Coating Performance.” *International Journal of Molecular Sciences* 16 (10): 24588–99. <https://doi.org/10.3390/ijms161024588>.
- Ashiuchi, Makoto, and Haruo Misono. 2003. “Poly-Gamma-Glutamic Acid.” In *Biopolymers: Volume 7 - Polyamides and Complex Proteinaceous Materials I*, edited by S. R. Fahnestock and A. Steinbüchel, 123–73. WILEY-VCH.
- Ashiuchi, Makoto, Chizuko Nawa, Tohru Kamei, Jae-Jun Song, Seung-Pyo Hong, Moon-Hee Sung, Kenji Soda, Toshiharu Yagi, and Haruo Misono. 2001. “Physiological and Biochemical Characteristics of Poly  $\gamma$ -Glutamate Synthetase Complex of *Bacillus Subtilis*.” *European Journal of Biochemistry* 268 (20): 5321–28. <https://doi.org/10.1046/j.0014-2956.2001.02475.x>.
- Ashiuchi, Makoto, Kenji Soda, and Haruo Misono. 1999. “A Poly- $\gamma$ -Glutamate Synthetic System of *Bacillus Subtilis* IFO 3336: Gene Cloning and Biochemical Analysis of Poly- $\gamma$ -Glutamate Produced by *Escherichia Coli* Clone Cells.” *Biochemical and Biophysical Research Communications* 263 (1): 6–12.
- Ashiuchi, Makoto, Daisuke Yamashiro, and Kento Yamamoto. 2013. “*Bacillus Subtilis* EdmS (Formerly PgsE) Participates in the Maintenance of Episomes.” *Plasmid* 70 (2): 209–15. <https://doi.org/10.1016/j.plasmid.2013.03.008>.
- Barun, K. De, Sandra L. Bragg, Gary N. Sanden, Kathy E. Wilson, Lois A. Diem, Chung K. Marston, Alex R. Hoffmaster, et al. 2002. “Two-Component Direct Fluorescent-Antibody Assay for Rapid Identification of *Bacillus Anthracis*.” *Emerging Infectious Diseases* 8 (10):

1060–65. <https://doi.org/10.3201/eid0810.020392>.

Bosso, Antonella, Loretta Panero, Maurizio Petrozziello, Marco Sollazzo, Andriani Asproudi, Silvia Motta, and Massimo Guaita. 2015. “Use of Polyaspartate as Inhibitor of Tartaric Precipitations in Wines.” *Food Chemistry* 185: 1–6. <https://doi.org/10.1016/j.foodchem.2015.03.099>.

Candela, Thomas, and Agnès Fouet. 2005. “Bacillus Anthracis CapD, Belonging to the  $\gamma$ -Glutamyltranspeptidase Family, Is Required for the Covalent Anchoring of Capsule to Peptidoglycan.” *Molecular Microbiology* 57 (3): 717–26. <https://doi.org/10.1111/j.1365-2958.2005.04718.x>.

———. 2006. “Poly-Gamma-Glutamate in Bacteria.” *Molecular Microbiology* 60 (5): 1091–98. <https://doi.org/10.1111/j.1365-2958.2006.05179.x>.

Cao, Mingfeng, Weitao Geng, Li Liu, Cunjiang Song, Hui Xie, Wenbin Guo, Yinghong Jin, and Shufang Wang. 2011. “Glutamic Acid Independent Production of Poly- $\gamma$ -Glutamic Acid by Bacillus Amyloliquefaciens LL3 and Cloning of *PgsBCA* Genes.” *Bioresource Technology* 102 (5): 4251–57. <https://doi.org/10.1016/j.biortech.2010.12.065>.

Cao, Mingfeng, Weitao Geng, Wei Zhang, Jibin Sun, Shufang Wang, Jun Feng, Ping Zheng, Anna Jiang, and Cunjiang Song. 2013. “Engineering of Recombinant *Escherichia Coli* Cells Co-Expressing Poly- $\gamma$ -Glutamic Acid ( $\gamma$ -PGA) Synthetase and Glutamate Racemase for Differential Yielding of  $\gamma$ -PGA.” *Microbial Biotechnology* 6 (6): 675–84. <https://doi.org/10.1111/1751-7915.12075>.

- Cao, Mingfeng, Cunjiang Song, Yinghong Jin, Li Liu, Jing Liu, Hui Xie, Wenbin Guo, and Shufang Wang. 2010. "Synthesis of Poly ( $\gamma$ -Glutamic Acid) and Heterologous Expression of *PgsBCA* Genes." *Journal of Molecular Catalysis B: Enzymatic* 67 (1–2): 111–16. <https://doi.org/10.1016/j.molcatb.2010.07.014>.
- Carlos, Joseph L., Mark Paetzel, Philip A. Klenotic, Natalie C J Strynadka, and Ross E. Dalbey. 2001. "Bacterial Type I Signal Peptidases." In *The Enzymes*, 22:27–55. [https://doi.org/10.1016/S1874-6047\(02\)80003-8](https://doi.org/10.1016/S1874-6047(02)80003-8).
- Dammeyer, Thorben, and Philip Tinnefeld. 2012. "Engineered Fluorescent Proteins Illuminate the Bacterial Periplasm." *Computational and Structural Biotechnology Journal* 3 (4): e201210013. <https://doi.org/10.5936/csbj.201210013>.
- Dementin, Sébastien, Ahmed Bouhss, Geneviève Auger, Claudine Parquet, Dominique Mengin-Lecreulx, Otto Dideberg, Jean Van Heijenoort, and Didier Blanot. 2001. "Evidence of a Functional Requirement for a Carbamoylated Lysine Residue in MurD, MurE and MurF Synthetases as Established by Chemical Rescue Experiments." *European Journal of Biochemistry* 268 (22): 5800–5807. <https://doi.org/10.1046/j.0014-2956.2001.02524.x>.
- Dobson, László, István Reményi, and Gábor E. Tusnády. 2015. "CCTOP: A Consensus Constrained TOPology Prediction Web Server." *Nucleic Acids Research* 43: W408–12. <https://doi.org/10.1093/nar/gkv451>.
- Dörr, Jonas M., Stefan Scheidelaar, Martijn C. Koorengel, Juan J. Dominguez, Marre Schäfer, Cornelis A. van Walree, and J. Antoinette Killian. 2016. "The Styrene–Maleic Acid

Copolymer: A Versatile Tool in Membrane Research.” *European Biophysics Journal* 45 (1): 3–21. <https://doi.org/10.1007/s00249-015-1093-y>.

Drew, David, Dan Sjöstrand, Johan Nilsson, Thomas Urbig, Chen Ni Chin, Jan Willem De Gier, and Gunnar Von Heijne. 2002. “Rapid Topology Mapping of Escherichia Coli Inner-Membrane Proteins by Prediction and PhoA/GFP Fusion Analysis.” *Proceedings of the National Academy of Sciences of the United States of America* 99 (5): 2690–95. <https://doi.org/10.1073/pnas.052018199>.

Feng, Jun, Weixia Gao, Yanyan Gu, Wei Zhang, Mingfeng Cao, Cunjiang Song, Peng Zhang, Min Sun, Chao Yang, and Shufang Wang. 2014. “Functions of Poly-Gamma-Glutamic Acid ( $\gamma$ -PGA) Degradation Genes in  $\gamma$ -PGA Synthesis and Cell Morphology Maintenance.” *Applied Microbiology and Biotechnology* 98 (14): 6397–6407. <https://doi.org/10.1007/s00253-014-5729-0>.

Feng, Jun, Yanyan Gu, Yufen Quan, Mingfeng Cao, Weixia Gao, Wei Zhang, Shufang Wang, Chao Yang, and Cunjiang Song. 2015. “Improved Poly- $\gamma$ -Glutamic Acid Production in *Bacillus Amyloliquefaciens* by Modular Pathway Engineering.” *Metabolic Engineering* 32: 106–15. <https://doi.org/10.1016/j.ymben.2015.09.011>.

Feng, Jun, Yufen Quan, Yanyan Gu, Fenghong Liu, Xiaozhong Huang, Haosheng Shen, Yulei Dang, et al. 2017. “Enhancing Poly- $\gamma$ -Glutamic Acid Production in *Bacillus Amyloliquefaciens* by Introducing the Glutamate Synthesis Features from *Corynebacterium Glutamicum*.” *Microbial Cell Factories* 16 (1): 1–12. <https://doi.org/10.1186/s12934-017-0704-y>.

- Girasa, Emmanuel, and Marc De Wispelaere. 2003. "Polyaspartate, a New Alternative for the Conditioning of Cooling Water." *14th International Conference on the Properties of Water and Steam in Kyoto*, 587–93.
- Gübitz, Georg M, and Artur Cavaco Paulo. 2003. "New Substrates for Reliable Enzymes - Enzymatic Modification of Polymers." *Current Opinion in Biotechnology* 14 (6): 577–82.
- Halmschlag, Birthe, Xenia Steurer, Sastia P. Putri, Eiichiro Fukusaki, and Lars M. Blank. 2019. "Tailor-Made Poly- $\gamma$ -Glutamic Acid Production." *Metabolic Engineering* 55 (May): 239–48. <https://doi.org/10.1016/j.ymben.2019.07.009>.
- Hamano, Yoshimitsu. 2011. "Occurrence, Biosynthesis, Biodegradation, and Industrial and Medical Applications of a Naturally Occurring  $\epsilon$ -Poly-L-Lysine." *Bioscience, Biotechnology, and Biochemistry* 75 (7): 1226–33. <https://doi.org/10.1271/bbb.110201>.
- Hamano, Yoshimitsu, Toshinobu Arai, Makoto Ashiuchi, and Kuniki Kino. 2013. "NRPSs and Amide Ligases Producing Homopoly(Amino Acid)s and Homooligo(Amino Acid)S." *Natural Product Reports* 30 (8): 1087–97. <https://doi.org/10.1039/c3np70025a>.
- Holowka, Eric P, Victor Z Sun, Daniel T Kamei, and Timothy J Deming. 2007. "Polyarginine Segments in Block Copolypeptides Drive Both Vesicular Assembly and Intracellular Delivery." *Nature Materials* 6 (1): 52–57. <https://doi.org/10.1038/nmat1794>.
- Hong, Seok Hoon, Yong-Chan Kwon, and Michael C. Jewett. 2014. "Non-Standard Amino Acid Incorporation into Proteins Using Escherichia Coli Cell-Free Protein Synthesis." *Frontiers in Chemistry* 2 (June): 1–7. <https://doi.org/10.3389/fchem.2014.00034>.

- Jang, Jeyoun, Minhui Cho, Hae Ri Lee, Kiweon Cha, Jeong Hoon Chun, Kee Jong Hong, Jungchan Park, and Gi Eun Rhie. 2013. “Monoclonal Antibody against the Poly- $\gamma$ -d-Glutamic Acid Capsule of *Bacillus Anthracis* Protects Mice from Enhanced Lethal Toxin Activity Due to Capsule and Anthrax Spore Challenge.” *Biochimica et Biophysica Acta - General Subjects* 1830 (3): 2804–12. <https://doi.org/10.1016/j.bbagen.2012.11.006>.
- Jiang, Hao, Longan Shang, Sung H. Yoon, Sang Y. Lee, and Ziniu Yu. 2006. “Optimal Production of Poly-Gamma-Glutamic Acid by Metabolically Engineered *Escherichia Coli*.” *Biotechnology Letters* 28 (16): 1241–46. <https://doi.org/10.1007/s10529-006-9080-0>.
- Jiménez-Guerrero, I, M Cubo, F Pérez-Montaña, F López-Baena, B Guash-Vidal, F Ollero, R Bellogín, and M Espuny. 2013. *Bacterial Protein Secretion Systems. Beneficial Plant-Microbial Interactions*. <https://doi.org/10.1201/b15251-10>.
- Ju, Wan Taek, Yong Su Song, Woo Jin Jung, and Ro Dong Park. 2014. “Enhanced Production of Poly- $\gamma$ -Glutamic Acid by a Newly-Isolated *Bacillus Subtilis*.” *Biotechnology Letters* 36 (11): 2319–24. <https://doi.org/10.1007/s10529-014-1613-3>.
- Karimova, Gouzel, and Daniel Ladant. 2017. “Defining Membrane Protein Topology Using *Pho-Lac* Reporter Fusions.” In *Bacterial Protein Secretion Systems. Methods in Molecular Biology, Vol 1615.*, edited by L. Journet and E. Cascales, 129–42. New York, NY: Humana Press.
- Ke, Na, Dirk Landgraf, Johan Paulsson, and Mehmet Berkmen. 2016. “Visualization of Periplasmic and Cytoplasmic Proteins with a Self-Labeling Protein Tag.” *Journal of*

- Bacteriology* 198 (7): 1035–43. <https://doi.org/10.1128/JB.00864-15>.
- Kihara, Daisuke. 2017. *Protein Function Prediction*. Vol. 1611. <https://doi.org/10.1007/978-1-4939-7015-5>.
- Kimura, Keitarou, Lam Son Phan Tran, Ikuo Uchida, and Yoshifumi Itoh. 2004. “Characterization of *Bacillus Subtilis*  $\gamma$ -Glutamyltransferase and Its Involvement in the Degradation of Capsule Poly- $\gamma$ -Glutamate.” *Microbiology* 150 (12): 4115–23. <https://doi.org/10.1099/mic.0.27467-0>.
- Kino, Kuniki, Toshinobu Arai, and Yasuhiro Arimura. 2011. “Poly- $\alpha$ -Glutamic Acid Synthesis Using a Novel Catalytic Activity of RimK from *Escherichia Coli* K-12.” *Applied and Environmental Microbiology* 77 (6): 2019–25. <https://doi.org/10.1128/AEM.02043-10>.
- Kolayarattil, Meera B. 2013. “Sec-Dependent Protein Translocation in *Escherichia Coli* : Biochemical Analysis of Interactions between SecA , Signal Peptidase and Signal Peptides.” University of Connecticut - Storrs.
- Kreyenschulte, Dirk, Rainer Krull, and Argyrios Margaritis. 2014. “Recent Advances in Microbial Biopolymer Production and Purification.” *Critical Reviews in Biotechnology* 34 (1): 1–15. <https://doi.org/10.3109/07388551.2012.743501>.
- Lee, Jeong Wook, Hyun Uk Kim, Sol Choi, Jongho Yi, and Sang Yup Lee. 2011. “Microbial Production of Building Block Chemicals and Polymers.” *Current Opinion in Biotechnology* 22 (6): 758–67. <https://doi.org/10.1016/j.copbio.2011.02.011>.
- Liu, C. L., H. G. Dong, K. Xue, W. Yang, P. Liu, D. Cai, X. Liu, Y. Yang, and Z. Bai. 2019.

- “Biosynthesis of Poly- $\gamma$ -Glutamic Acid in *Escherichia Coli* by Heterologous Expression of PgsBCAE Operon from *Bacillus*.” *Journal of Applied Microbiology* 128: 1390–99. <https://doi.org/10.1111/jam.14552>.
- Makino, S. I., I. Uchida, N. Terakado, C. Sasakawa, and M. Yoshikawa. 1989. “Molecular Characterization and Protein Analysis of the *Cap* Region, Which Is Essential for Encapsulation in *Bacillus Anthracis*.” *Journal of Bacteriology* 171 (2): 722–30.
- Manocha, Bhavik, and Argyrios Margaritis. 2010. “A Novel Method for the Selective Recovery and Purification of  $\gamma$ -Polyglutamic Acid from *Bacillus Licheniformis* Fermentation Broth.” *Biotechnology Progress* 26 (3): 734–42. <https://doi.org/10.1002/btpr.370>.
- Matsumoto, Ken’ichiro, and Seiichi Taguchi. 2013. “Enzyme and Metabolic Engineering for the Production of Novel Biopolymers: Crossover of Biological and Chemical Processes.” *Current Opinion in Biotechnology* 24 (6): 1054–60. <https://doi.org/10.1016/j.copbio.2013.02.021>.
- Munyendo, Were L L, Huixia Lv, Habiba Benza- Ingoula, Lilechi D Baraza, and Jianping Zhou. 2012. “Cell Penetrating Peptides in the Delivery of Biopharmaceuticals.” *Biomolecules* 2 (4): 187–202. <https://doi.org/10.3390/biom2020187>.
- Mutschler, Angela, Lorène Tallet, Morgane Rabineau, Camille Dollinger, Marie-Hélène Metz-Boutigue, Francis Schneider, Bernard Senger, Nihal Engin Vrana, Pierre Schaaf, and Philippe Lavalle. 2016. “Unexpected Bactericidal Activity of Poly(Arginine)/Hyaluronan Nanolayered Coatings.” *Chemistry of Materials* 28: 8700–8709.

<https://doi.org/10.1021/acs.chemmater.6b03872>.

Numata, Keiji. 2015. "Poly(Amino Acid)s/Polypeptides as Potential Functional and Structural Materials." *Polymer Journal* 47 (8): 537–45. <https://doi.org/10.1038/pj.2015.35>.

Ogunleye, Adetoro, Aditya Bhat, Victor U. Irorere, David Hill, Craig Williams, and Iza Radecka. 2015. "Poly- $\gamma$ -Glutamic Acid: Production, Properties and Applications." *Microbiology (Reading, England)* 161 (2015): 1–17. <https://doi.org/10.1099/mic.0.081448-0>.

Ojima, Yoshihiro, Joji Kobayashi, Takeru Doi, and Masayuki Azuma. 2019. "Knockout of *PgdS* and *Ggt* Gene Changes Poly- $\gamma$ -Glutamic Acid Production in *Bacillus Licheniformis* RK14-46." *Journal of Biotechnology* 304: 57–62. <https://doi.org/10.1016/j.jbiotec.2019.08.003>.

Park, Chung, Jae Chul Choi, Yoon Ho Choi, Hisaaki Nakamura, Kazuya Shimanouchi, Terumi Horiuchi, Haruo Misono, et al. 2005. "Synthesis of Super-High-Molecular-Weight Poly- $\gamma$ -Glutamic Acid by *Bacillus Subtilis* Subsp. *Chungkookjang*." *Journal of Molecular Catalysis B: Enzymatic* 35 (4–6): 128–33. <https://doi.org/10.1016/j.molcatb.2005.06.007>.

Postis, Vincent, Shaun Rawson, Jennifer K. Mitchell, Sarah C. Lee, Rosemary A. Parslow, Tim R. Dafforn, Stephen A. Baldwin, and Stephen P. Muench. 2015. "The Use of SMALPs as a Novel Membrane Protein Scaffold for Structure Study by Negative Stain Electron Microscopy." *Biochimica et Biophysica Acta - Biomembranes* 1848 (2): 496–501. <https://doi.org/10.1016/j.bbamem.2014.10.018>.

Pugsley, A P. 1993. "The Complete General Secretory Pathway in Gram-Negative Bacteria." *Microbiological Reviews* 57 (1): 50–108.

<http://www.ncbi.nlm.nih.gov/pubmed/8096622><http://www.pubmedcentral.nih.gov/articlerender.fcgi?artid=PMC372901>.

Reynolds, Elinor, Jeremy I. Ross, and Jonathan H. Cove. 2003. "Msr(A) and Related Macrolide/Streptogramin Resistance Determinants: Incomplete Transporters?" *International Journal of Antimicrobial Agents* 22 (3): 228–36. [https://doi.org/10.1016/S0924-8579\(03\)00218-8](https://doi.org/10.1016/S0924-8579(03)00218-8).

Ross, Jeremy I., E. Anne Eady, Jonathan H. Cove, and Simon Baumberg. 1995. "Identification of a Chromosomally Encoded ABC-Transport System with Which the Staphylococcal Erythromycin Exporter MsrA May Interact." *Gene* 153 (1): 93–98. [https://doi.org/10.1016/0378-1119\(94\)00833-E](https://doi.org/10.1016/0378-1119(94)00833-E).

Sambrook, J, and D W Russell. 2001. *Molecular Cloning - A Laboratory Manual - Vol. 1, 2 and 3*. Third Edit. New York: Cold Spring Harbor Laboratory Press.

Schwede, Torsten, Jürgen Kopp, Nicolas Guex, and Manuel C. Peitsch. 2003. "SWISS-MODEL: An Automated Protein Homology-Modeling Server." *Nucleic Acids Research* 31 (13): 3381–85. <https://doi.org/10.1093/nar/gkg520>.

Scoffone, Viola, Daniele Dondi, Ginevra Biino, Giovanni Borghese, Dario Pasini, Alessandro Galizzi, and Cinzia Calvio. 2013. "Knockout of *PgdS* and *Ggt* Genes Improves  $\gamma$ -PGA Yield in *B. Subtilis*." *Biotechnology and Bioengineering* 110 (7): 2006–12. <https://doi.org/10.1002/bit.24846>.

Shi, Feng, Zhinan Xu, and Peilin Cen. 2007. "Microbial Production of Natural Poly Amino Acid."

- Science in China, Series B: Chemistry* 50 (3): 291–303. <https://doi.org/10.1007/s11426-007-0061-5>.
- Shih, Ing Lung, Ming Haw Shen, and Yi Tsong Van. 2006. “Microbial Synthesis of Poly( $\epsilon$ -Lysine) and Its Various Applications.” *Bioresource Technology* 97 (9): 1148–59. <https://doi.org/10.1016/j.biortech.2004.08.012>.
- Sievers, Fabian, Andreas Wilm, David Dineen, Toby J. Gibson, Kevin Karplus, Weizhong Li, Rodrigo Lopez, et al. 2011. “Fast, Scalable Generation of High-Quality Protein Multiple Sequence Alignments Using Clustal Omega.” *Molecular Systems Biology* 7 (539). <https://doi.org/10.1038/msb.2011.75>.
- Smith, Clyde A. 2006. “Structure, Function and Dynamics in the Mur Family of Bacterial Cell Wall Ligases.” *Journal of Molecular Biology* 362 (4): 640–55. <https://doi.org/10.1016/j.jmb.2006.07.066>.
- Soto, Ana Maria, and David Draper. 2012. “White Gels: An Easy Way to Preserve Methylene Blue Stained Gels.” *Analytical Biochemistry* 421 (1): 345–46. <https://doi.org/10.1016/j.ab.2011.10.048>.
- Soye, Benjamin J. Des, Jaymin R. Patel, Farren J. Isaacs, and Michael C. Jewett. 2015. “Repurposing the Translation Apparatus for Synthetic Biology.” *Current Opinion in Chemical Biology* 28: 83–90. <https://doi.org/10.1016/j.cbpa.2015.06.008>.
- Szczepanek, Susanne, Mihai Cikala, and Charles N David. 2002. “Poly-Gamma-Glutamate Synthesis during Formation of Nematocyst Capsules in *Hydra*.” *Journal of Cell Science* 115

(Pt 4): 745–51. <http://www.ncbi.nlm.nih.gov/pubmed/11865030>.

- Tarui, Yutaka, Hanako Iida, Eiichiro Ono, Wataru Miki, Eiji Hirasawa, Ken Ichi Fujita, Toshio Tanaka, and Makoto Taniguchi. 2005. “Biosynthesis of Poly- $\gamma$ -Glutamic Acid in Plants: Transient Expression of Poly- $\gamma$ -Glutamate Synthetase Complex in Tobacco Leaves.” *Journal of Bioscience and Bioengineering* 100 (4): 443–48. <https://doi.org/10.1263/jbb.100.443>.
- Tian, Guangming, Juntao Fu, Xuetao Wei, Zhixia Ji, Xin Ma, Gaofu Qi, and Shouwen Chen. 2014. “Enhanced Expression of *PgdS* Gene for High Production of Poly- $\gamma$ -Glutamic Acid with Lower Molecular Weight in *Bacillus Licheniformis* WX-02.” *Journal of Chemical Technology and Biotechnology* 89: 1825–32. <https://doi.org/10.1002/jctb.4261>.
- Troy, Frederic A. 1973. “Chemistry and Biosynthesis of the Poly (  $\gamma$ -D-Glutamyl ) Capsule in *Bacillus Licheniformis*.” *Journal of Biological Chemistry* 248 (1): 305–15.
- Tsuge, Yota, Hideo Kawaguchi, Kengo Sasaki, and Akihiko Kondo. 2016. “Engineering Cell Factories for Producing Building Block Chemicals for Bio-Polymer Synthesis.” *Microbial Cell Factories* 15 (1): 19. <https://doi.org/10.1186/s12934-016-0411-0>.
- Urushibata, Yuji, Shinji Tokuyama, and Yasutaka Tahara. 2002. “Characterization of the *Bacillus Subtilis* *YwsC* Gene, Involved in Gamma-Polyglutamic Acid Production.” *Journal of Bacteriology* 184 (2): 337–43. <https://doi.org/10.1128/JB.184.2.337>.
- Wang, N, G Yang, C Che, and Y Liu. 2011. “Heterogenous Expression of Poly-Gamma-Glutamic Acid Synthetase Complex Gene of *Bacillus Licheniformis* WBL-3.” *Applied Biochemistry and Microbiology* 47 (4): 381–85. <https://doi.org/10.1134/s0003683811040193>.

- Wang, Q., X. Wei, and S. Chen. 2017. *Production and Application of Poly- $\gamma$ -Glutamic Acid. Current Developments in Biotechnology and Bioengineering*. Elsevier B.V. <https://doi.org/10.1016/B978-0-444-63662-1.00030-0>.
- Weber, Jakob. 1995. "The Development of Cnidarian Stinging Cells: Maturation and Migration of Stenoteles of *Hydra Vulgaris*." *Roux's Archives of Developmental Biology* 205 (3–4): 171–81. <https://doi.org/10.1007/BF00357763>.
- Xavier, Janifer Raj, Mrithula Mahalakshmi Madhan Kumarr, Gopalan Natarajan, Karna Venkata Ramana, and Anil Dutt Semwal. 2019. "Optimized Production of Poly ( $\gamma$ -Glutamic Acid) ( $\gamma$ -PGA) Using *Bacillus Licheniformis* and Its Application as Cryoprotectant for Probiotics." *Biotechnology and Applied Biochemistry*, 1–12. <https://doi.org/10.1002/bab.1879>.
- Xu, Guoqiang, Jian Zha, Hui Cheng, Mohammad H.A. Ibrahim, Fan Yang, Hunter Dalton, Rong Cao, et al. 2019. "Engineering *Corynebacterium Glutamicum* for the de Novo Biosynthesis of Tailored Poly- $\gamma$ -Glutamic Acid." *Metabolic Engineering* 56 (May): 39–49. <https://doi.org/10.1016/j.ymben.2019.08.011>.
- Yamaguchi, Fumio, Yoshihiro Ogawa, Mamoru Kikuchi, Katsumi Yuasa, and Hiroshi Motai. 1996. "Detection of  $\gamma$ -Polyglutamic Acid ( $\gamma$ -PGA) by SDS-Page." *Bioscience, Biotechnology, and Biochemistry* 60 (2): 255–58. <https://doi.org/10.1271/bbb.60.255>.
- Yamashiro, Daisuke, Yutaka Minouchi, and Makoto Ashiuchi. 2011. "Moonlighting Role of a Poly- $\gamma$ -Glutamate Synthetase Component from *Bacillus Subtilis*: Insight into Novel Extrachromosomal DNA Maintenance." *Applied and Environmental Microbiology* 77 (8):

2796–98. <https://doi.org/10.1128/AEM.02649-10>.

Yamashiro, Daisuke, Megumi Yoshioka, and Makoto Ashiuchi. 2011. “*Bacillus Subtilis PgsE* (Formerly *YwtC*) Stimulates Poly- $\gamma$ -Glutamate Production in the Presence of Zinc.” *Biotechnology and Bioengineering* 108 (1): 226–30. <https://doi.org/10.1002/bit.22913>.

Yoon, Sung Ho, Jin Hwan Do, Sang Yup Lee, and Ho Nam Chang. 2000. “Production of Poly- $\gamma$  - Glutamic Acid by Fed-Batch Culture of *Bacillus Licheniformis*.” *Time*, no. Lee 1996: 585–88.

Zeng, Wei, Guiguang Chen, Yunkai Zhang, Kongyang Wu, and Zhiqun Liang. 2012. “Studies on the UV Spectrum of Poly( $\gamma$ -Glutamic Acid) Based on Development of a Simple Quantitative Method.” *International Journal of Biological Macromolecules* 51 (1–2): 83–90. <https://doi.org/10.1016/j.ijbiomac.2012.04.005>.